

Supplementary Information

Phototriggered Formation and Disappearance of Surface-Confined Self-Assembly Composed of Photochromic 2-Thienyl-Type Diarylethene: A Cooperative Model at the Liquid/Solid Interface

Soichi Yokoyama, Takashi Hirose and Kenji Matsuda*

Department of Synthetic Chemistry and Biological Chemistry, Graduate School of Engineering, Kyoto University, Katsura, Nishikyo-ku, Kyoto 615-8510, Japan

E-mail: kmatsuda@sbchem.kyoto-u.ac.jp

Contents:

Experimental Details

A. Syntheses of Materials	S1
B. UV-vis. Spectroscopy and Photochemical Reaction	S5
C. STM Measurements	S5
D. Molecular Modeling	S5
E. Langmuir Adsorption-Based Cooperative Assembly Model on 2-D Surface	S5

Supporting Data

Fig. S1 UV-vis spectral change of 1 in CH ₂ Cl ₂ and octanoic acid upon photoisomerization	S8
Fig. S2 Another high resolution STM images of 1o at octanoic acid/HOPG interface	S9
Fig. S3 STM image of 1o at various concentrations	S10
Fig. S4 Histograms of surface coverage of 1o around the critical concentration	S11
Fig. S5 STM images of 1o at high concentrations (> 750 μM)	S12
Fig. S6 Histograms of domain sizes of 1o on HOPG surface at high concentrations (> 750 μM)	S13
Fig. S7 The plot of average domain size over concentration of 1o	S14
Fig. S8 Concentration dependence of the fractional coverage of 1c at the octanoic acid/HOPG interface	S15
Fig. S9 Dependence of conversion ratio of 1o on surface coverage on HOPG surface	S16
Fig. S10 Dependence of conversion ratio of 1o on surface coverage on HOPG surface	S17
Fig. S11 Molecular orientation of 1o in respect to the HOPG lattice	S18
Fig. S12-S23 ¹ H and ¹³ C NMR spectra of compounds 5–7 and 1–3	S19

References

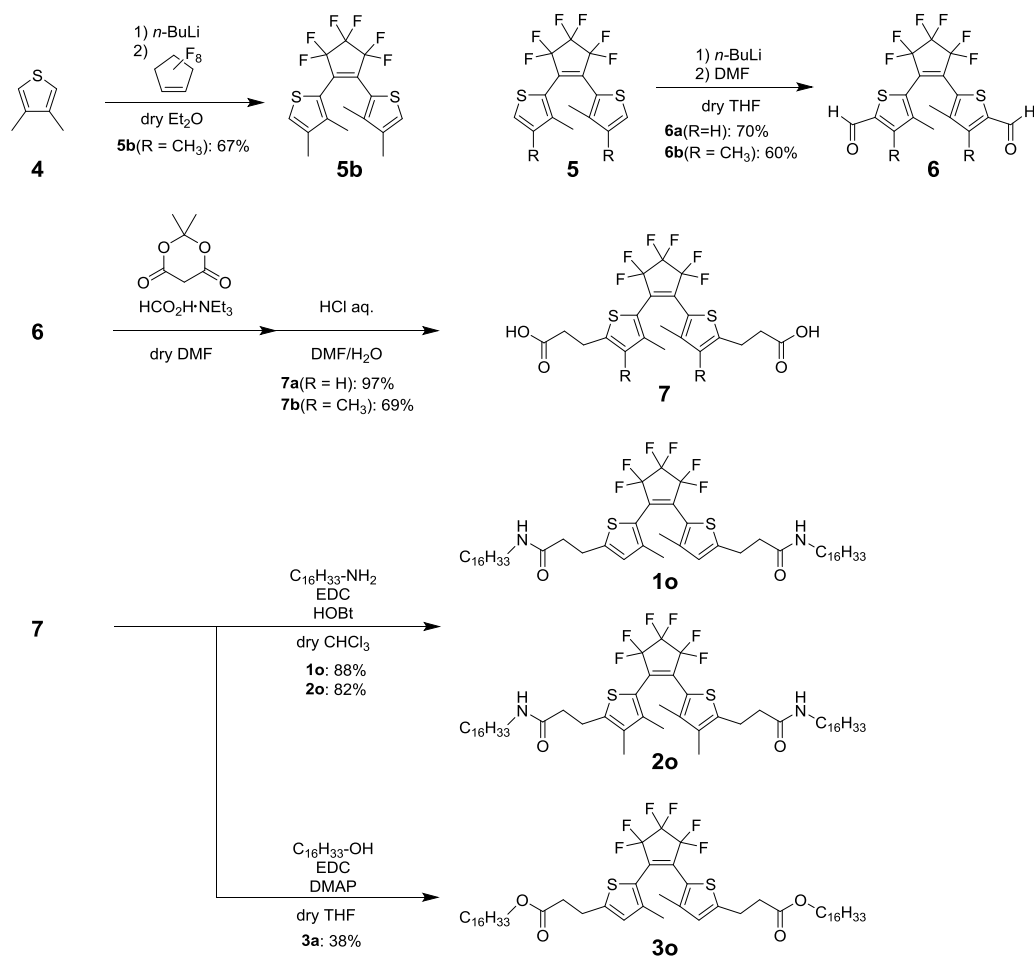
S31

Experimental details

A. Syntheses of the materials

General. Unless specifically mentioned, reagents and solvents were obtained from commercial suppliers and used without further purification. All reactions were monitored by thin-layer chromatography carried out on 0.2 mm Merck silica gel plates (60F-254). Column chromatography was performed on silica gel (Nakarai Tesque, 70-230 mesh for normal phase or 75C18-OPN, 75 μ m for reverse phase) or on a Biotage Instrument (Isolera One) with a SNAP flash silica gel cartridge (KP-Sil). Final product was purified by a preparative gel permeation chromatography (GPC) (Japan Analytical Industry Co., Ltd., JAIGEL-1H and 2H). ^1H and ^{13}C NMR spectra were recorded on a JEOL JMN-A500 or JNM-ECA600 instruments. Proton and carbon chemical shifts are reported in ppm downfield from tetramethylsilane (TMS). Mass spectra were obtained by a Thermo Scientific LTQ orbitrapXL mass spectrometer. IR spectra were recorded on a Jasco FT/IR-4200 equipped with an ATR detector PRO450-S (Ge crystal). *N,N*-dimethylformamide was dried with calcium hydride and distilled before use. Compounds **4**^{S1} and **5a**^{S2} have been prepared according to a literature procedure. Triethyl ammonium formic acid (TEAF) was prepared as follows: triethylamine (16.2 g, 0.16 mol) was slowly added dropwise to formic acid (18.4 g, 0.40 mol) during cooling and stirring.^{S3}

Scheme S1. Synthesis of **1o**, **2o**, and **3o**



Synthesis of 1,2-bis(3,4-dimethyl-2-thienyl)hexafluorocyclopentene (5b)

To a solution of 3,4-dimethylthiophene **4**^{S1} (5.61 g, 50.0 mmol) in dry Et₂O (150 mL) was slowly added dropwise *n*-BuLi (1.6 M in hexanes, 32.0 mL, 51.2 mmol) at 0 °C under nitrogen atmosphere for 30 min. The mixture was stirred at room temperature for 30 min and refluxed for 30 min. The resulting mixture was cooled to 0 °C. Then perfluorocyclopentene (3.3 mL, 25 mmol) was added by a cooled syringe for 30 min under nitrogen atmosphere with keeping below 10 °C. After stirring at 0 °C for 1 h, the reaction was quenched by an addition of aq. HCl (1 N, 50 mL). The mixture was extracted with Et₂O and combined organic layers were dried over MgSO₄, filtered, and evaporated. The crude product was purified by silica gel column chromatography (hexane) to give a yellow solid **5b** (6.57 g, 16.6 mmol, 67%).

5b: ¹H NMR (500 MHz, CDCl₃): δ 1.66 (s, 6H), 2.08 (s, 6H), 7.11 (s, 2H); IR (Ge ATR, neat): ν_{max} 2952, 1607, 1472, 1441, 1376, 1335, 1266, 1191, 1161, 1110, 1056 cm⁻¹; HRMS (MALDI-orbitrap) *m/z* [M]⁺ calcd for C₁₇H₁₄F₆O₄S₂⁺: 396.0436, found: 396.0426.

Synthesis of 1,2-bis(5-formyl-3-methyl-2-thienyl)hexafluorocyclopentene (6a)

To a solution of **5a**^{S2} (10.0 g, 27.2 mmol) in dry THF (100 mL) was slowly added dropwise *n*-BuLi (1.6 M in hexanes, 37.5 mL, 60.0 mmol) at -78 °C under nitrogen atmosphere. The mixture was stirred at -78 °C for 30 min and further stirred at 0 °C for 30 min. After addition of *N,N*-dimethylformamide (1.0 mL, 13 mmol) at 0 °C by one portion, the reaction mixture was stirred at room temperature for 1 h. The reaction was quenched with aq. HCl (12 N, 3.0 mL). The reaction product was extracted with Et₂O twice, and combined organic layers were washed with brine, dried over MgSO₄, filtered, and evaporated. The crude product was purified by silica gel column chromatography (gradient eluting from hexane/CH₂Cl₂ = 1/1 to CH₂Cl₂) to give a yellow solid. The solid was recrystallized from hexane to yield a pale yellow solid **6a** (8.08 g, 19.0 mmol, 70%).

6a: ¹H NMR (500 MHz, CDCl₃): δ 1.91 (s, 6H), 7.52 (s, 2H), 9.88 (s, 2H); IR (Ge ATR, neat): ν_{max} 1667, 1539, 1455, 1394, 1342, 1272, 1231, 1198, 1158, 1127, 1067, 1037, 1011 cm⁻¹; HRMS (MALDI-orbitrap) *m/z* [M + H]⁺ calcd for C₁₇H₁₁F₆O₂S₂⁺: 425.0099, found: 425.0104.

Synthesis of 1,2-bis(3,4-dimethyl-5-formyl-2-thienyl)hexafluorocyclopentene (6b)

To a solution of **5a** (0.500 g, 1.26 mmol) in dry THF (25 mL) was slowly added dropwise *n*-BuLi (1.6 M in hexanes, 38 mL, 61 mmol) at 0 °C under nitrogen atmosphere. The mixture was stirred at 0 °C for 30 min and further stirred at room temperature for 20 min. After addition of *N,N*-dimethylformamide (8.0 mL, 100 mmol) at 0 °C by one portion, the reaction mixture was stirred at room temperature for 1 h. Then the reaction was quenched with aq. HCl (1 N, 10 mL). The reaction product was extracted with Et₂O twice, and combined organic layers were washed with brine, dried over MgSO₄, filtered, and evaporated. The crude product was purified by silica gel column chromatography (gradient eluting from hexane/CH₂Cl₂ = 1/1 to CH₂Cl₂) to give a yellow solid **6b** (0.341 g, 0.754 mmol, 60%).

6b: ¹H NMR (500 MHz, CDCl₃): δ 1.80 (s, 6H), 2.43 (s, 6H), 1.99 (quint, *J* = 6.5 Hz, 2H), 10.07 (s, 2H); IR (Ge ATR, neat): ν_{max} 1682, 1663, 1271, 1238, 1196, 1057 cm⁻¹; HRMS (MALDI-orbitrap) *m/z* [M + H]⁺ calcd for C₁₉H₁₅F₆O₂S₂⁺: 453.0412, found: 453.0414.

Synthesis of 1,2-bis(5-(2-carboxyethyl)-3-methyl-2-thienyl)hexafluorocyclopentene (7a)

To a solution of **6a** (4.24 g, 10.0 mmol) in TEAF^{S3} (50 mL) and DMF (50 mL) was added Meldrum's acid (2.90 g, 20.1 mmol). The mixture was slowly heated to 100 °C over 1 h and was stirred for 5 h at the temperature. The resulting solution was then cooled to room temperature and the reaction was quenched by an addition of cooled water (100 g). The solution was acidified with concentrated aq. HCl until pH became 1. The reaction product was extracted with Et₂O. Combined organic layers were then extracted with aq. NaOH (1 N) and the aqueous layer was washed with Et₂O. The aqueous layer was again acidified with concentrated aq. HCl until pH became 1. The generated precipitates were collected by filtration, dried under reduced pressure to give a pale yellow solid **7a** (4.95 g, 9.65 mmol, 97%).

7a: ¹H NMR (500 MHz, CDCl₃): δ 2.02 (s, 6H), 2.67 (t, *J* = 6.5 Hz, 4H), 3.11 (t, *J* = 6.5 Hz, 4H), 6.61 (s, 2H); IR (Ge ATR, neat): ν_{\max} 1709, 1604, 1474, 1440, 1385, 1361, 1335, 1314, 1268, 1225, 1192, 1118, 1065 cm⁻¹; HRMS (MALDI-orbitrap) *m/z* [M]⁺ calcd for C₂₁H₁₈F₆O₄S₂⁺: 512.0545, found: 512.0546.

Synthesis of 1,2-bis(5-(2-carboxyethyl)-3,4-dimethyl-2-thienyl)hexafluorocyclopentene (7b)

To a solution of **6b** (0.274 g, 0.600 mmol) in TEAF^{S3} (5 mL) and DMF (5 mL) was added Meldrum's acid (0.174 g, 1.21 mmol). The mixture was stirred for 5 h at 100 °C. The resulting solution was then cooled to room temperature and the reaction was quenched by an addition of cooled water (10 g). The solution was acidified with concentrated aq. HCl until pH became 1. The reaction product was extracted with Et₂O and CH₂Cl₂. Combined organic layers were washed with water, dried over MgSO₄, filtered, and evaporated. The crude product was purified by silica gel column chromatography (CH₂Cl₂/MeOH = 9/1) and reversed phase chromatography (MeOH/H₂O = 7/3) to give a pale yellow solid **7b** (0.223 g, 0.413 mmol, 69%).

7b: ¹H NMR (500 MHz, CDCl₃): δ 2.93 (s, 6H), 2.00 (s, 6H), 2.65 (t, *J* = 7.0 Hz, 4H), 3.07 (t, *J* = 7.0 Hz, 4H), 8.78 (s, 2H); IR (Ge ATR, neat): ν_{\max} 2923, 2852, 1710, 1441, 1330, 1273, 1125 cm⁻¹; HRMS (MALDI-orbitrap) *m/z* [M]⁺ calcd for C₂₃H₂₂F₆N₂O₄S₂⁺: 540.0858, found 540.0860.

Synthesis of 1,2-bis(5-(N-hexadecyl-2-carbamoyl)ethyl)-3-methyl-2-thienyl)hexafluoropentene (1o)

To a dispersed solution of **7a** (0.205 g, 0.400 mmol) in dry CHCl₃ (20 mL) were added hexadecylamine (0.338 g, 1.40 mmol), 1-ethyl-3-(3-dimethylaminopropyl)carbodiimide hydrochloride (0.345 g, 1.80 mmol) and 1-hydroxybenzotriazole (0.111 g, 0.821 mmol). The mixture was stirred for 2 h at room temperature. The reaction mixture was extracted with CH₂Cl₂. Combined organic layers were washed with water, dried over MgSO₄, filtered, and evaporated. The crude product was purified by silica gel column chromatography (ethyl acetate/CHCl₃ = 4/1) to give a pale yellow solid **1o** (0.337 g, 0.352 mmol, 88%).

1o: ¹H NMR (500 MHz, CDCl₃): δ 0.88 (t, *J* = 7.0 Hz, 6H), 1.25-1.31 (m, 52H), 1.45 (quint, *J* = 6.7 Hz, 4H), 1.71 (s, 6H), 2.48 (t, *J* = 7.3 Hz, 4H), 3.12 (t, *J* = 7.3 Hz, 4H), 3.22 (q, *J* = 6.4 Hz, 4H), 5.56 (t, *J* = 5.5 Hz, 2H), 6.57 (s, 2H); ¹³C NMR (151MHz, CDCl₃): δ 14.1, 15.1, 22.6, 25.9, 26.9, 29.27, 29.32, 29.5, 29.57, 29.61, 29.7, 31.8, 37.9, 39.7, 108.9-12.8 (m), 115.6 (tt, *J* = 260 and 24Hz), 121.1, 128.8, 133.8 (t, *J* = 24 Hz), 141.1, 148.0, 170.9; IR (Ge ATR, neat): ν_{\max} 2959, 2919, 2850, 1634, 1468, 1384, 1271, 1191, 1130 cm⁻¹; HRMS (MALDI-orbitrap) *m/z* [M + H]⁺ calcd for C₅₃H₈₅F₆N₂O₂S₂⁺: 959.5951, found 959.5966; UV-vis (CH₂Cl₂): λ_{\max} (ϵ /M⁻¹cm⁻¹) 343(1.2 × 10⁴) nm.

Synthesis of 1,2-bis(3,4-dimethyl-5-(N-hexadecyl-2-carbamoyl)ethyl)-2-thienyl)hexafluorocyclopentene (2o)

To a dispersed solution of **7b** (0.200 g, 0.370 mmol) in dry CHCl₃ (20 mL) were added hexadecylamine (0.314 g, 1.30 mmol), 1-ethyl-3-(3-dimethylaminopropyl)carbodiimide hydrochloride (0.320 g, 1.67 mmol) and 1-hydroxybenzotriazole (0.100 g, 0.740 mmol). The mixture was stirred for 2 h at room temperature. The solvent was removed *in vacuo*, and then saturated NaHCO₃ aqueous solution was added to the residue. The reaction mixture was extracted with CH₂Cl₂, combined organic layers were washed with water, dried over MgSO₄, filtered, and evaporated. The crude product was purified by silica gel column chromatography (ethyl acetate/CHCl₃ = 4/1) to give a pale yellow solid **2o** (0.301 g, 0.305 mmol, 82%).

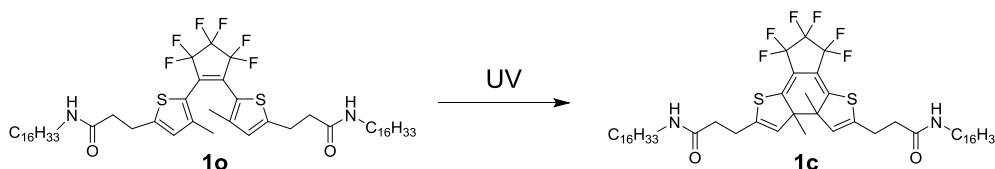
2o: ¹H NMR (500 MHz, CDCl₃): δ 0.88 (t, *J* = 6.5 Hz, 6H), 1.25-1.31 (m, 52H), 1.45 (quint, 6.5 Hz, 4H), 1.60 (s, 6H), 1.98 (s, 6H), 2.47 (t, *J* = 7.5 Hz, 4H), 3.10 (t, *J* = 7.5 Hz, 4H), 3.21 (q, *J* = 6.5 Hz, 4H), 5.65 (s, 2H); ¹³C NMR (151 MHz, CDCl₃): δ 12.5, 14.1, 14.2, 22.6, 24.3, 26.9, 29.26, 29.31, 29.50, 29.53, 29.56, 29.61, 29.65, 31.90, 37.5, 39.67, 108.9-112.8 (m), 115.7 (tt, *J* = 260 and 24 Hz), 119.7, 134.1, 134.2-134.4 (m), 140.9, 141.7, 171.0; IR (Ge ATR, neat): ν_{max} 3291, 2919, 2849, 1640, 1550, 1470, 1271, 1190, 1060 cm⁻¹; HRMS (MALDI-orbitrap) *m/z* [M + H]⁺ calcd for C₅₅H₈₉F₆N₂O₂S₂⁺: 987.6264, found 987.6268.

Synthesis of 1,2-bis(5-(1-hexadecylpropanate-3-yl)-3-methyl-2-thienyl)perfluorocyclopentene (3o)

To a solution of **7a** (0.256 g, 0.500 mmol) in dry THF (25 mL) were added hexadecanol (0.424 g, 1.75 mmol), 1-ethyl-3-(3-dimethylaminopropyl) carbodiimide hydrochlorid (0.211 g, 1.10 mmol), and 4-dimethylaminopyridine (DMAP) (61.1 mg, 0.500 mmol). The mixture was stirred for 2 days at room temperature. The reaction mixture was extracted with Et₂O. Combined organic layers were washed with aq. HCl (1 N) and saturated aq. NaHCO₃, dried over Na₂SO₄, filtrated, and evaporated. The crude product was purified by silica gel column chromatography (CH₂Cl₂/hexane = 1:1) to give a pale yellow solid **3o** (0.185 g, 0.192 mmol, 38%).

3o: ¹H NMR (500 MHz, CDCl₃): δ 0.88 (t, *J* = 7.0 Hz, 6H), 1.26-1.30 (m, 52H), 1.61 (quint, *J* = 7.5 Hz, 4H), 1.67 (s, 6H), 2.66 (t, 4H), 3.09 (t, *J* = 7.5 Hz, 4H), 4.08 (t, *J* = 6.8 Hz, 4H), 6.57 (s, 1H); ¹³C NMR (151 MHz, CDCl₃): δ 14.1, 15.1, 22.7, 25.3, 25.9, 28.6, 29.2, 29.3, 29.5, 29.6, 29.62, 29.64, 29.7, 31.9, 35.6, 64.9, 110.8 (tquint, *J* = 270 and 25 Hz), 115.6 (tt, 260 and 24 Hz), 121.3, 128.6, 133.8 (t, *J* = 24 Hz) 141.1, 147.4, 172.0; IR (Ge ATR, neat): ν_{max} 2916, 2850, 1734, 1473, 1363, 1341, 1275, 1187, 1122, 1065 cm⁻¹; HRMS (MALDI-orbitrap) *m/z* [M]⁺ calcd for C₅₃H₈₃F₆O₄S₂⁺: 960.5553, found: 960.5557

Synthesis of 4,9-bis(N-hexadecyl-2-carbamoyl)ethyl)-6,7-dimethyl-13,13,14,14,15,15-hexafluorotetracyclo[10.3.0.0(2,6).0(7,11)]-3,10-dithiapentadeca-1,4,8,11-tetraene (1c)



In a quartz flask, a solution of **1o** (100 mg) in acetone was irradiated by UV light (365 nm) for 1 h with stirring. The solvent was evaporated *in vacuo*. The mixture was isolated by silica gel column chromatography (ethyl acetate/CHCl₃ = 1/1) in a dark room to give an orange solid **1c** (25 mg, 0.10 mmol, 25 %).

1c: ^1H NMR (500 MHz, CDCl_3): δ 0.88 (t, $J = 7.3$ Hz, 6H), 1.25-1.28 (m, 52H), 1.34 (s, 6H), 1.48 (quint, $J = 7.0$ Hz, 4H), 2.37 (t, $J = 7.3$ Hz, 4H), 2.64-2.75 (m, 4H), 3.17-3.28 (m, 4H), 5.37 (s, 2H), 5.43 (t, $J = 5.5$ Hz, 2H); HRMS (MALDI-orbitrap) m/z $[\text{M} + \text{H}]^+$ calcd for $\text{C}_{53}\text{H}_{85}\text{F}_6\text{N}_2\text{O}_2\text{S}_2^+$: 959.5951, found 959.5938; UV-vis (CH_2Cl_2): λ_{max} ($\epsilon/\text{M}^{-1}\text{cm}^{-1}$) 436 (6.3×10^3) nm.

B. UV-vis. Spectroscopy and Photochemical Reaction

Absorption spectra were measured on a spectrophotometer (HITACHI U-3310). Optical length of the quartz cells were 10 mm or 2.0 mm. Photoirradiation experiments on HOPG surface were performed by a MUV-202U (MORITEX Co.) Xe/Hg lamp with a sharp cut filter (UV-29) and bandpass filter (U340) for UV light (0.64 W/cm^2 , $\lambda = 290\text{-}360$ nm), and with sharp cut filters (U-29 and Y-44) for visible light (0.32 W/cm^2 , $\lambda > 440$ nm). Conversion-ratio determined solutions of **1o** were prepared by a USHIO 500 W super high pressure mercury lamp with combination of a thermal cut, sharp cut (U-29), and bandpass filters (U330).

C. STM measurement

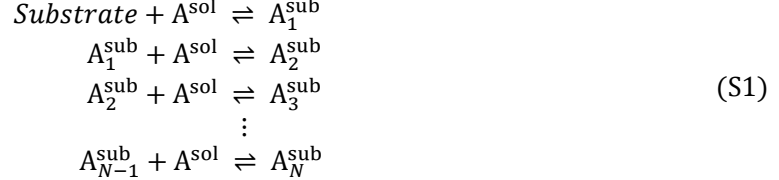
All STM experiments were performed at room temperature and ambient conditions. The STM images were acquired with a PicoSPM instrument (Molecular Imaging co.) or an Agilent technologies 5500 scanning probe microscopes in the constant current mode. The STM tips used in this research were mechanically cut from a Pt/Ir (80/20, diameter 0.25 mm) wire. Highly oriented pyrolytic graphite (HOPG) (purchased from the Bruker Co.) was used as a substrate. Solutions of **1o** and **1c** in 1-octanoic acid for the STM measurements were prepared by mixing into the solvent under heating. A drop of the solution (8-10 μL) was deposited onto freshly cleaved HOPG, and the tip was immersed into the solution and then the image was scanned. STM images were analyzed by using the graphite substrate as a calibration grid. For the experiment of the dependence of surface coverage on conversion ratio, a mother solution of diarylethene **1o** in octanoic acid were prepared at a concentration of 400 μM . The conversion ratio of sample solutions were determined by absorption spectra after ex situ UV irradiation. Surface coverage at each conversion ratio was obtained from the STM image of the sample whose conversion ratio was predetermined. The total area of STM image was $1.0 \times 10^7 \text{ nm}^2$ in the region of conversion ratio at which the change of surface coverage is prominent (i.e. from 40 to 60 %) and $5.0 \times 10^6 \text{ nm}^2$ in the region of the other concentration.

D. Molecular Modeling

The molecular ordering adsorbed on HOPG surface was modeled by a molecular mechanics/molecular dynamics (MM/MD) approach using Materials Studio v6.1.0, Accelrys Software Inc. The Dreiding force field implemented in the Forcite module was used for MM and MD calculations. The initial geometries were inspired from experimentally observed high resolution STM images for each ordering. For HOPG substrate, only one layer of graphene sheet (C-C bond length is 1.42 Å, flat geometry having hexagonal symmetry) was assumed. The Cartesian position of the graphene sheet was fixed during MM/MD calculations to suppress deformation/distortion of substrate.

E. Langmuir Adsorption-Based Cooperative Assembly Model on 2-D Surface

In order to simulate a monolayer formation of organic compound at a liquid/solid interface, this model is based on the Langmuir adsorption model in which uniform active sites are assumed. Inspired by cooperative self-assembly model in a solution (i.e. K_2 - K model),^{S4} we assumed two processes for ordering formation having different equilibrium constants; an initial nucleation on a substrate described by the nucleation constant K_n followed by subsequent stepwise elongation processes described by the elongation constant K_e .



At the nucleation step in eqn (S1), a molecule in a supernatant solution, A^{sol} , adsorbs on substrate making a nucleus on the substrate, A_1^{sub} . The rate of nucleation is proportional to the number of active sites (i.e. $(1 - \theta) \frac{A_{\text{sub}}}{S}$) and concentration in supernatant solution (i.e. $[A^{\text{sol}}]$), while the rate of desorption of the nuclei A_1^{sub} is proportional to the number of nuclei on surface (i.e. $[A_1^{\text{sub}}]LN_A$). Therefore temporal differentiation of $[A_1^{\text{sub}}]$ is given by:

$$\frac{d[A_1^{\text{sub}}]}{dt} = k_n \cdot (1 - \theta) \frac{A_{\text{sub}}}{S} \cdot [A^{\text{sol}}] - k_{-n} \cdot [A_1^{\text{sub}}]LN_A \tag{S2}$$

where k_n and k_{-n} are nucleation rate constants of adsorption and desorption whose units are $M^{-1}s^{-1}$ and s^{-1} , respectively, θ is fractional coverage of surface area, A_{sub} is the total area of substrate, S is occupied area by a molecular component A on surface, L is volume of supernatant solution, and N_A is Avogadro constant. By considering the number of active sites and nuclei in the temporal differentiation, we can deal with the adsorption/desorption rate constants equivalently. Assuming steady-state approximation, $[A_1^{\text{sub}}]$ is given by:

$$[A_1^{\text{sub}}] = \frac{(1 - \theta) A_{\text{sub}}}{LN_A S} K_n [A^{\text{sol}}] \tag{S3}$$

where nucleation constant K_n is defined as the ratio of k_n/k_{-n} . Since the subsequent elongation process in eqn (S1) is described as incremental addition of monomer from supernatant solution to N -mer domain, following differential equations are satisfied:

$$\begin{aligned}
 \frac{d[A_2^{\text{sub}}]}{dt} &= k_e \cdot [A_1^{\text{sub}}]LN_A \cdot [A^{\text{sol}}] - k_{-e} \cdot [A_2^{\text{sub}}]LN_A \\
 &\vdots \\
 \frac{d[A_N^{\text{sub}}]}{dt} &= k_e \cdot [A_{N-1}^{\text{sub}}]LN_A \cdot [A^{\text{sol}}] - k_{-e} \cdot [A_N^{\text{sub}}]LN_A
 \end{aligned} \tag{S4}$$

where k_e and k_{-e} are elongation rate constants of adsorption and desorption whose units are $M^{-1}s^{-1}$ and s^{-1} , respectively. Assuming steady-state approximation, the molar concentration of N -mer domains on substrate is given by:

$$[A_N^{\text{sub}}] = \frac{(1 - \theta) A_{\text{sub}}}{LN_A S} \sigma (K_e [A^{\text{sol}}])^N \tag{S5}$$

where elongation constant K_e is defined as the ratio of k_e/k_{-e} and the parameter of σ is degree of cooperativity defined as the ratio of K_n/K_e , the latter of which is smaller than unity for a cooperative process. Note that eqn (S3) can be observed from eqn (S5) by substituting N with 1. The total molar concentration of component A on the substrate, c_t^{sub} , is given by:

$$\begin{aligned}
c_t^{\text{sub}} &= [A_1^{\text{sub}}] + 2[A_2^{\text{sub}}] + 3[A_3^{\text{sub}}] + \dots + N[A_N^{\text{sub}}] + \dots \\
&= \sum_{i=1}^{\infty} i \cdot \frac{(1-\theta) A_{\text{sub}}}{LN_A S} \sigma (K_e [A^{\text{sol}}])^i \\
&= \frac{(1-\theta) A_{\text{sub}}}{LN_A S} \frac{\sigma K_e [A^{\text{sol}}]}{(1 - K_e [A^{\text{sol}}])^2}
\end{aligned} \tag{S6}$$

where $K_e [A^{\text{sol}}] < 1$ is assumed to approximate the form of infinite series. Concentration change in supernatant solution upon the adsorption/desorption events is taken into account by introducing the mass balance equation (S6) and the volume of supernatant solution L in this model. Since the fractional coverage θ is the ratio of the occupied area with component A to the total area of substrate, θ is given by:

$$\theta = \frac{c_t^{\text{sub}} \cdot L \cdot N_A \cdot S}{A_{\text{sub}}} \tag{S7}$$

Combining eqns (S6) and (S7) yields eqn (S8):

$$\theta = (1 - \theta) \frac{\sigma K_e [A^{\text{sol}}]}{(1 - K_e [A^{\text{sol}}])^2} \tag{S8}$$

Total concentration of A in the system, c_t , is given by:

$$c_t = [A^{\text{sol}}] + c_t^{\text{sub}} \tag{S9}$$

Combining eqns (S7) and (S9) yields eqn (S10)

$$c_t = [A^{\text{sol}}] + \alpha \theta, \text{ where } \alpha = \frac{A_{\text{sub}}}{L \cdot N_A \cdot S} \tag{S10}$$

The simultaneous equations of (S8) and (S10) gives eqn (S11):

$$\theta = (1 - \theta) \frac{\sigma K_e (c_t - \alpha \theta)}{\{1 - K_e (c_t - \alpha \theta)\}^2} \tag{S11}$$

In this model simulation, the values of L , S , and A_{sub} were experimentally determined (e.g. $L = 1.0 \times 10^{-6}$ L, $S = 3.1 \times 10^{-18}$ m², and $A_{\text{sub}} = 1.44 \times 10^{-4}$ m²), therefore α was treated as a constant. When c_t , K_e , and σ are given, θ is derived from the eqn (S11). The dependence of fractional coverage θ on the total concentration of **10** was experimentally observed by STM measurements. To obtain a curve of best fit for the experimental plot, K_e and σ were optimized by a non-linear regression analysis implemented in MATLAB® software (R2013a, version 8.1.0.604, win64) so that the residual error between experimental values of θ over c_t and the simulated values is minimized. In the concentration region at which $K_e [A^{\text{sol}}] \geq 1$, a complete coverage was assumed in the model simulation.

Supporting Data

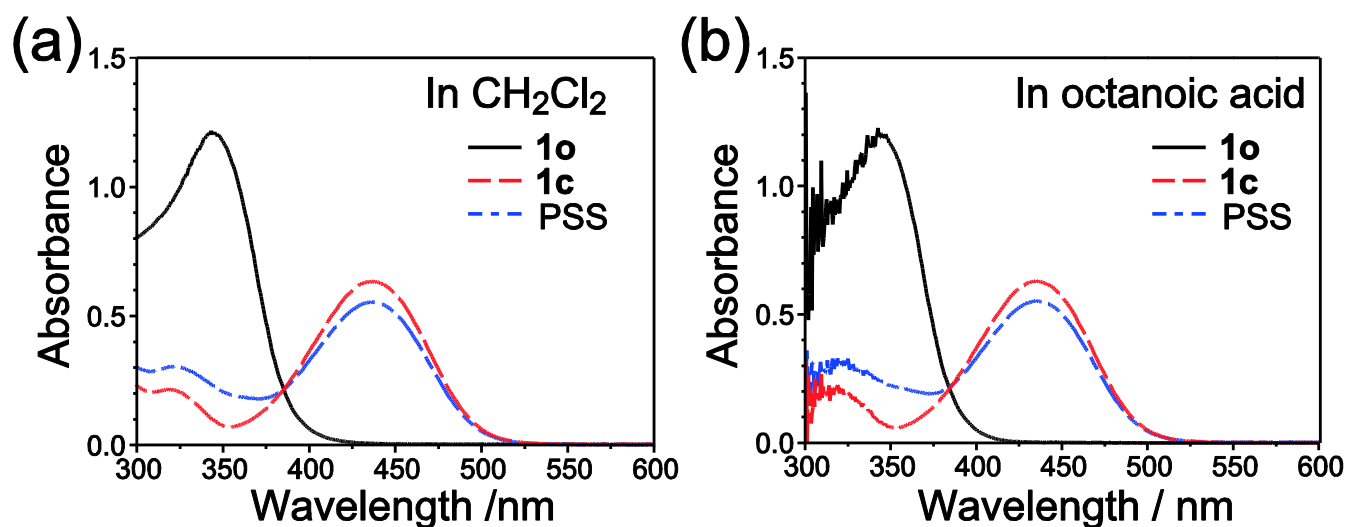


Fig. S1 UV-vis spectral change of **1** (a) in CH₂Cl₂ and (b) in octanoic acid upon photoisomerization ($c = 1 \times 10^{-4}$ M). Black solid line denotes the open-ring isomer, red dashed line denotes the closed-ring isomer, and blue dotted line denotes the sample at the photostationary state (PSS) upon UV (365 nm) irradiation. Upon UV irradiation at 365 nm to a solution of **1o** in CH₂Cl₂, new absorption band appeared at ~ 436 nm with an isobestic point. Successive visible light irradiation ($\lambda > 450$ nm) regenerated the original spectrum of the open-ring isomer. The conversion ratio of the open- to the closed-ring isomer of **1** was 12:88 both in CH₂Cl₂ and octanoic acid at the photostationary state (PSS) under the UV irradiation at 365 nm.

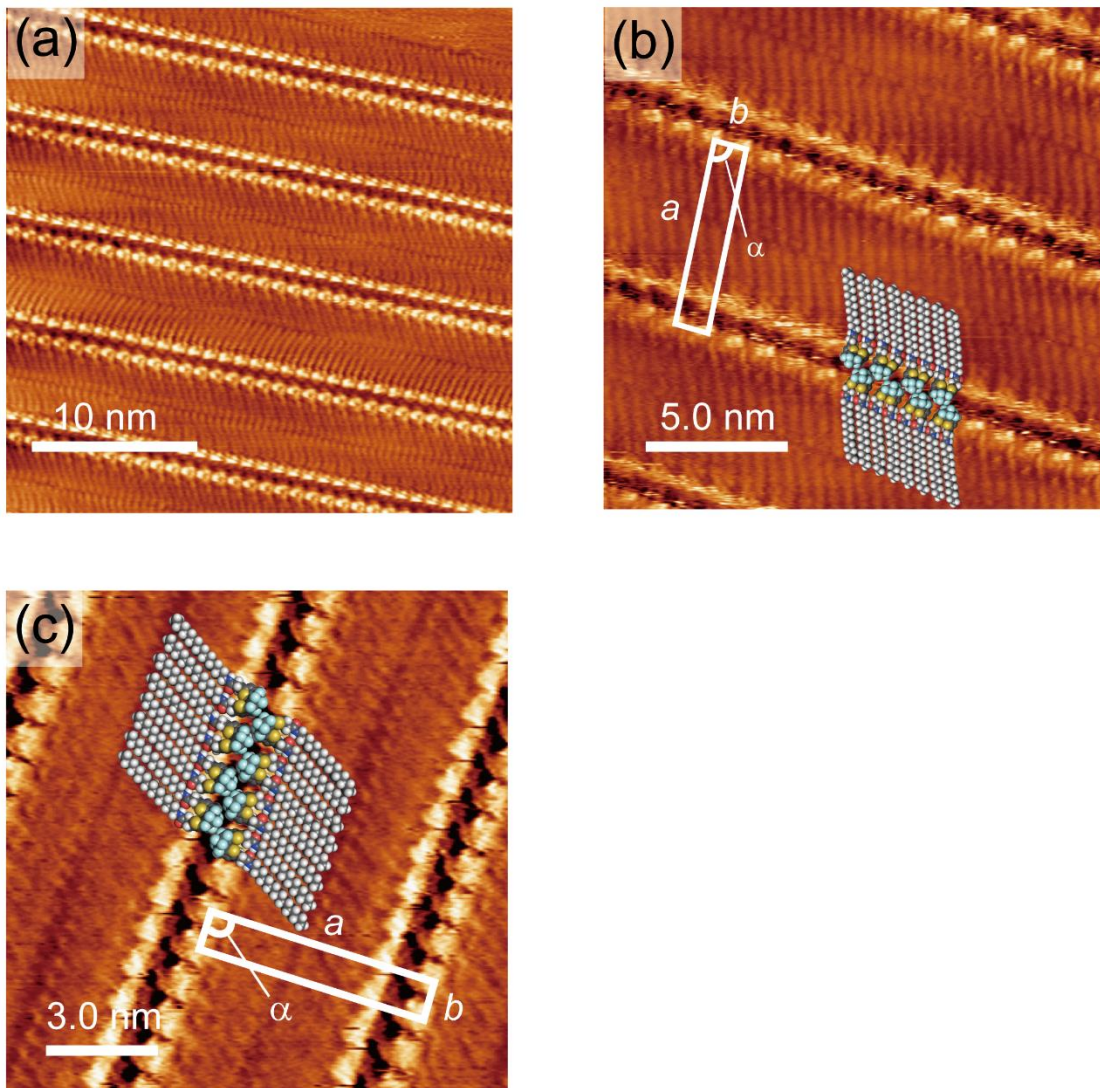


Fig. S2 Another STM images of **1o** at the octanoic acid/HOPG interface in different scales ($I_{\text{set}} = 30$ pA, $V_{\text{bias}} = 800$ mV, $a = 6.3$ nm, $b = 1.0$ nm, $\alpha = 89^\circ$). Two alkyl chains of a diarylethene **1o** can be clearly seen in these STM images.

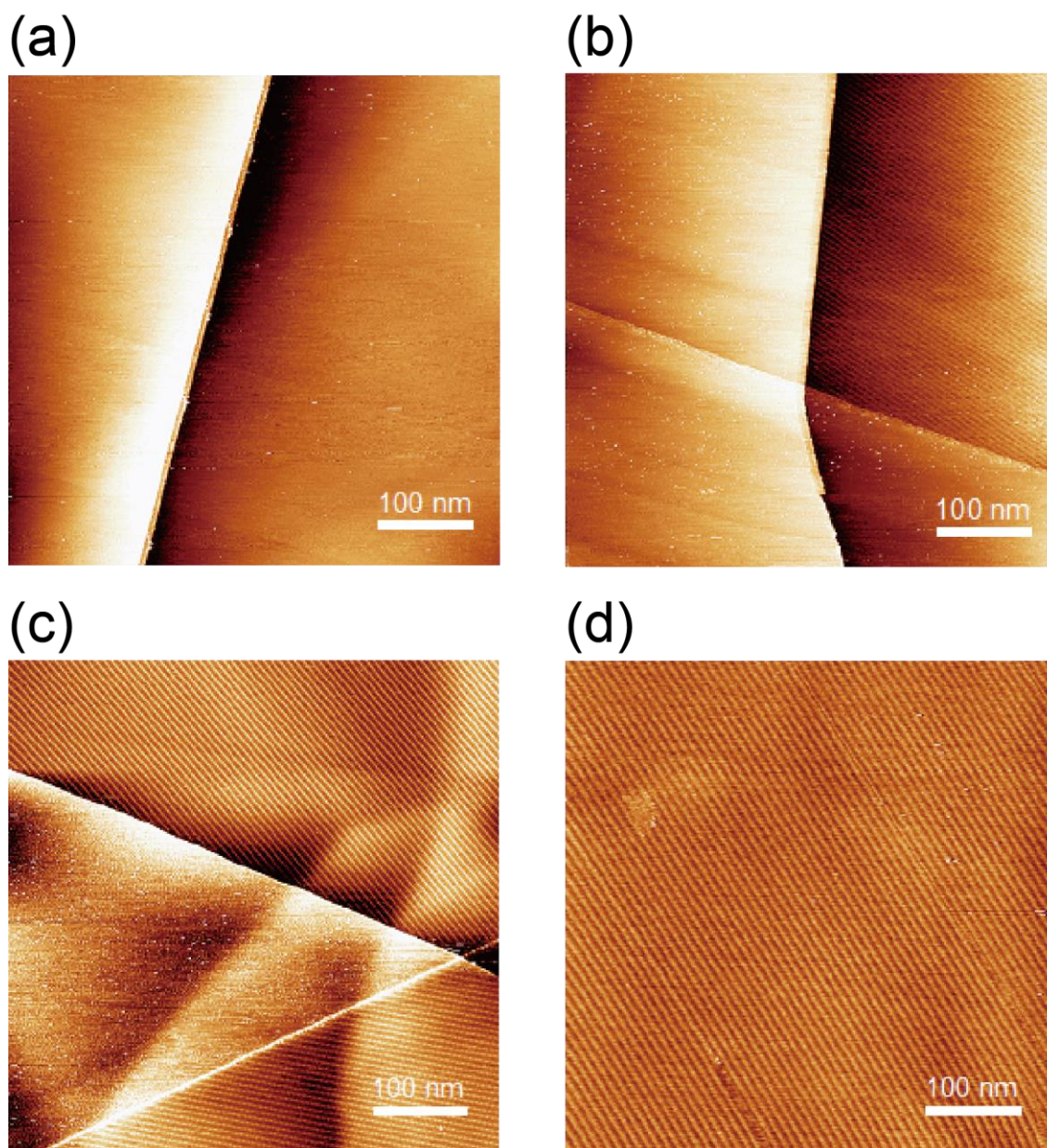


Fig. S3 Concentration dependent STM images of **1o** at octanoic acid/HOPG interface. The concentration of **1o** solution were (a) 200 μM , (b) 210 μM , (c) 220 μM and (d) 240 μM , respectively.

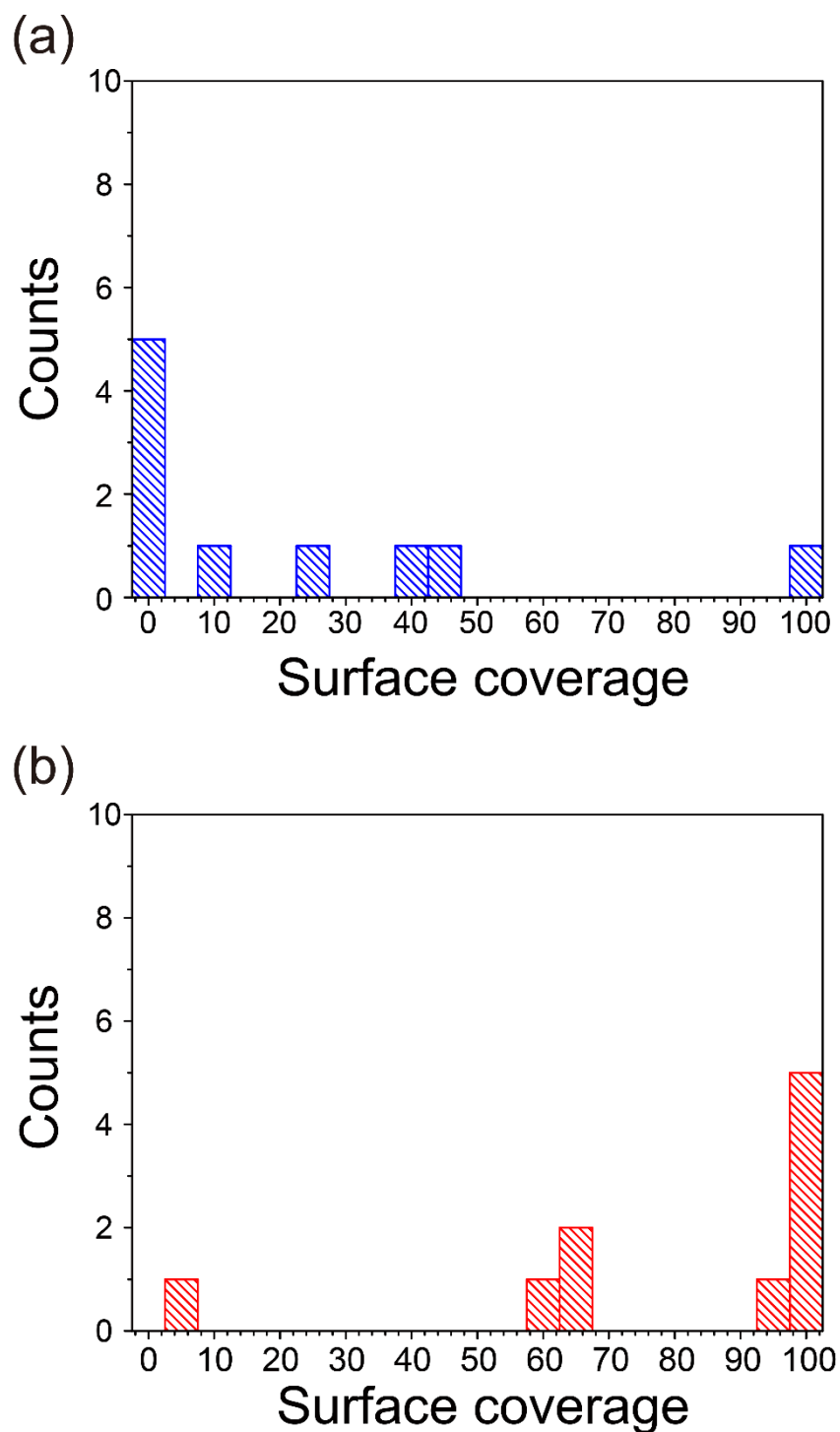


Fig. S4 Histograms of surface coverage of **1o** on HOPG surface around the critical concentration ($\sim 200 \mu\text{M}$) at (a) $210 \mu\text{M}$ and (b) $220 \mu\text{M}$. The total area of STM image was $1.0 \times 10^7 \text{ nm}^2$ in the region of concentration at which the change of surface coverage is prominent (i.e. from 210 to $230 \mu\text{M}$).

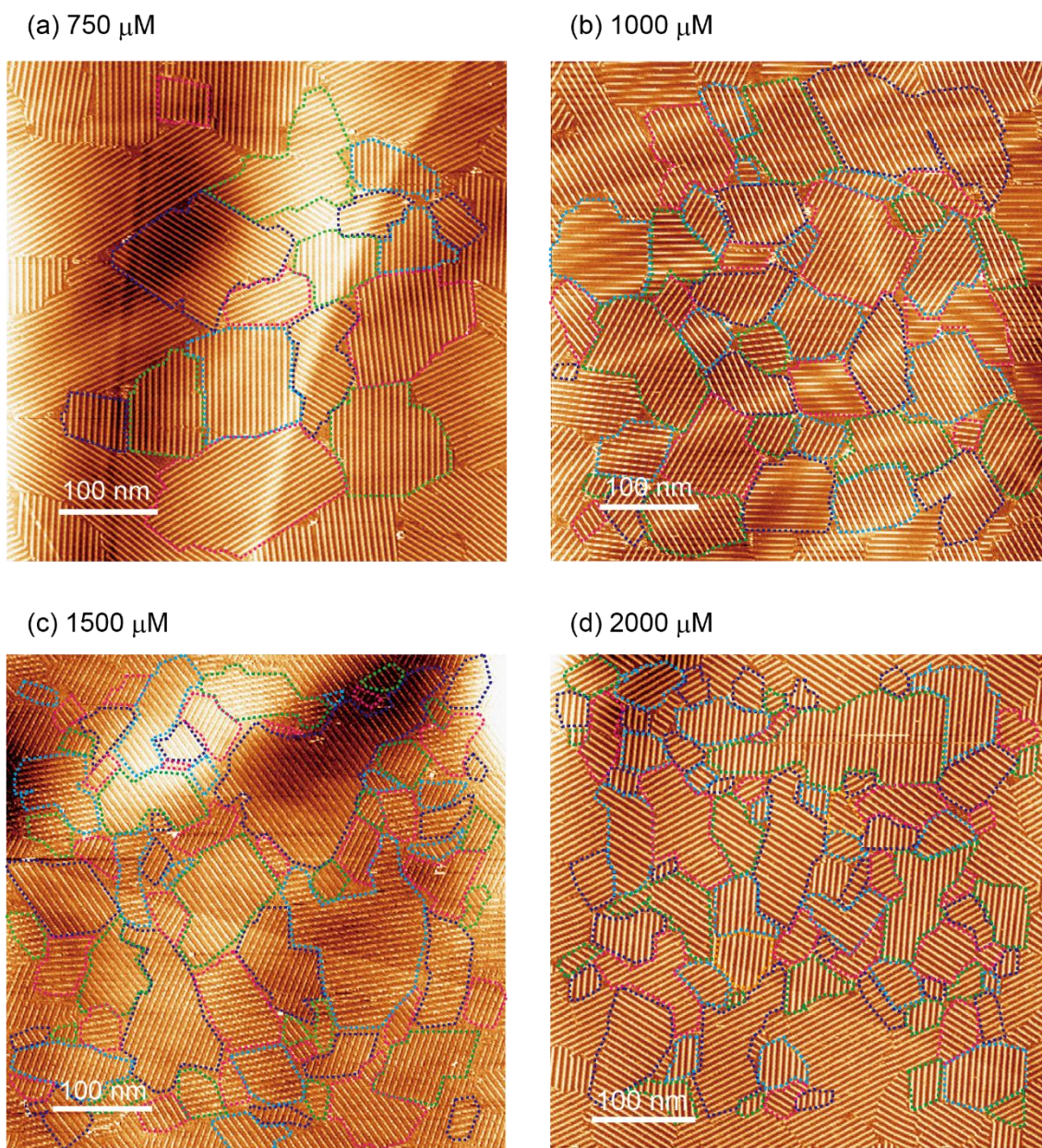


Fig. S5 STM images of **1o** at octanoic acid/HOPG interface at high concentrations ($> 750 \mu\text{M}$). The concentration of **1o** were (a) 750 μM , (b) 1000 μM , (c) 1500 μM and (d) 2000 μM . The domains marked by colored dotted lines were counted on a histogram. The other domains contacting with edge of images were eliminated due to unclear domain size.

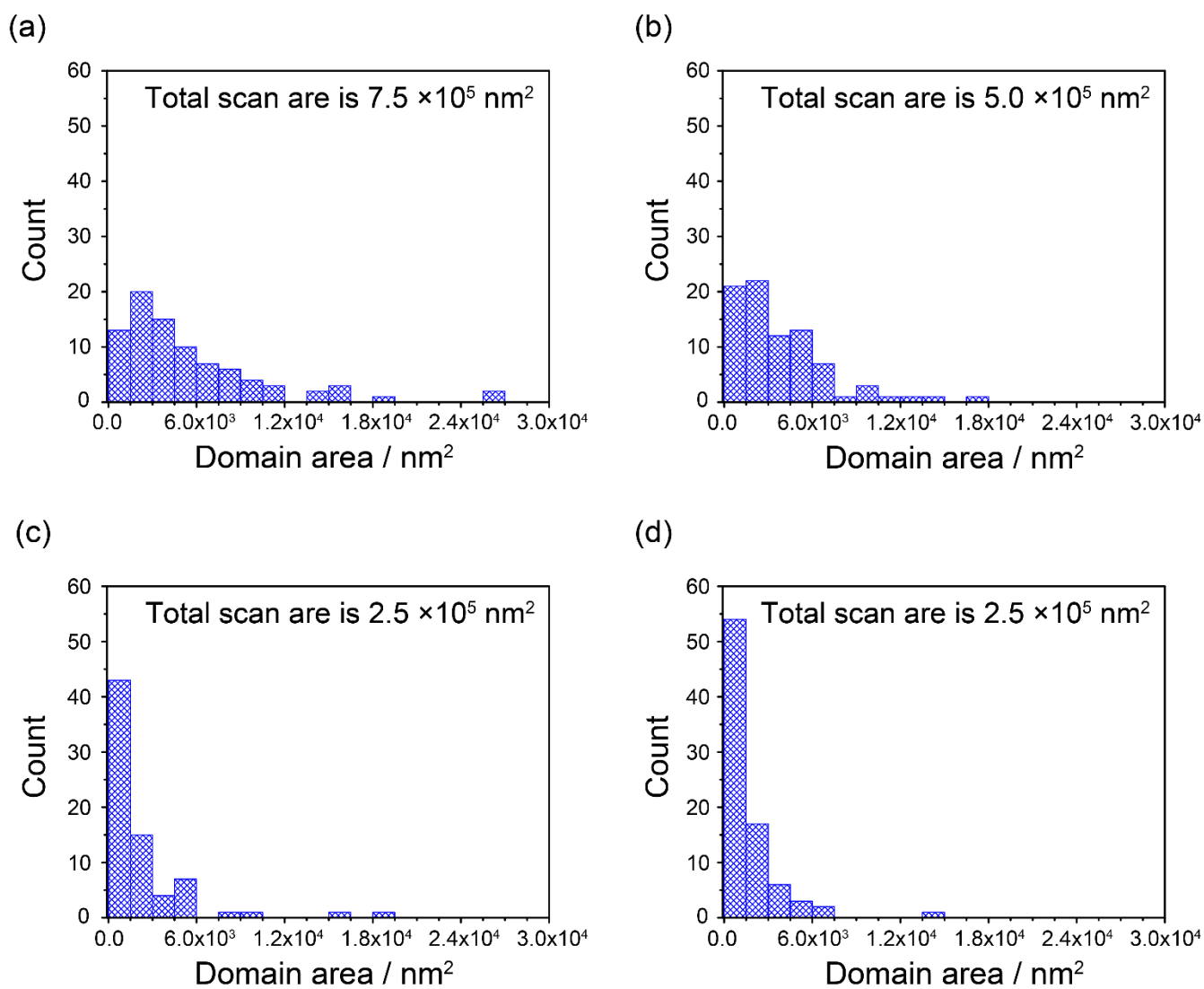


Fig. S6 Histograms of domain areas of **1o** on HOPG surface at high concentrations ($> 750 \mu\text{M}$). Concentrations of **1o** were (a) $750 \mu\text{M}$, (b) $1000 \mu\text{M}$, (c) 1500 and (d) $2000 \mu\text{M}$. The total area of STM image was shown in the graph.

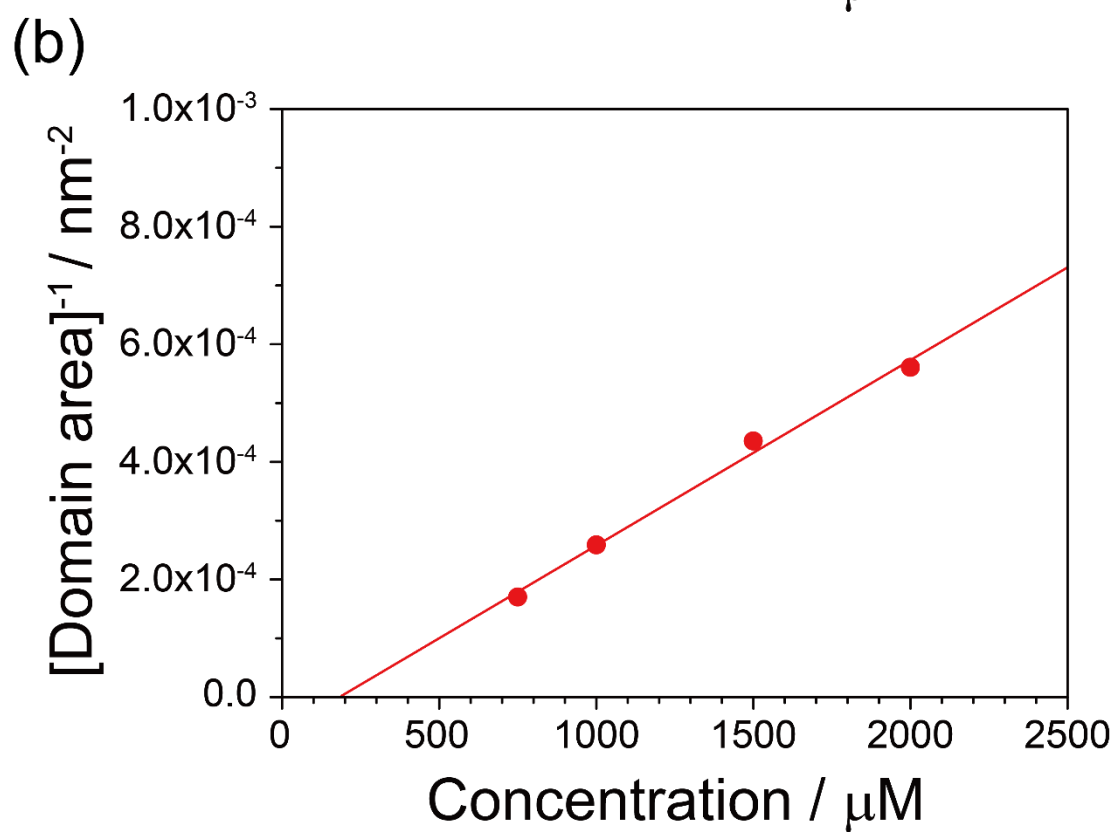
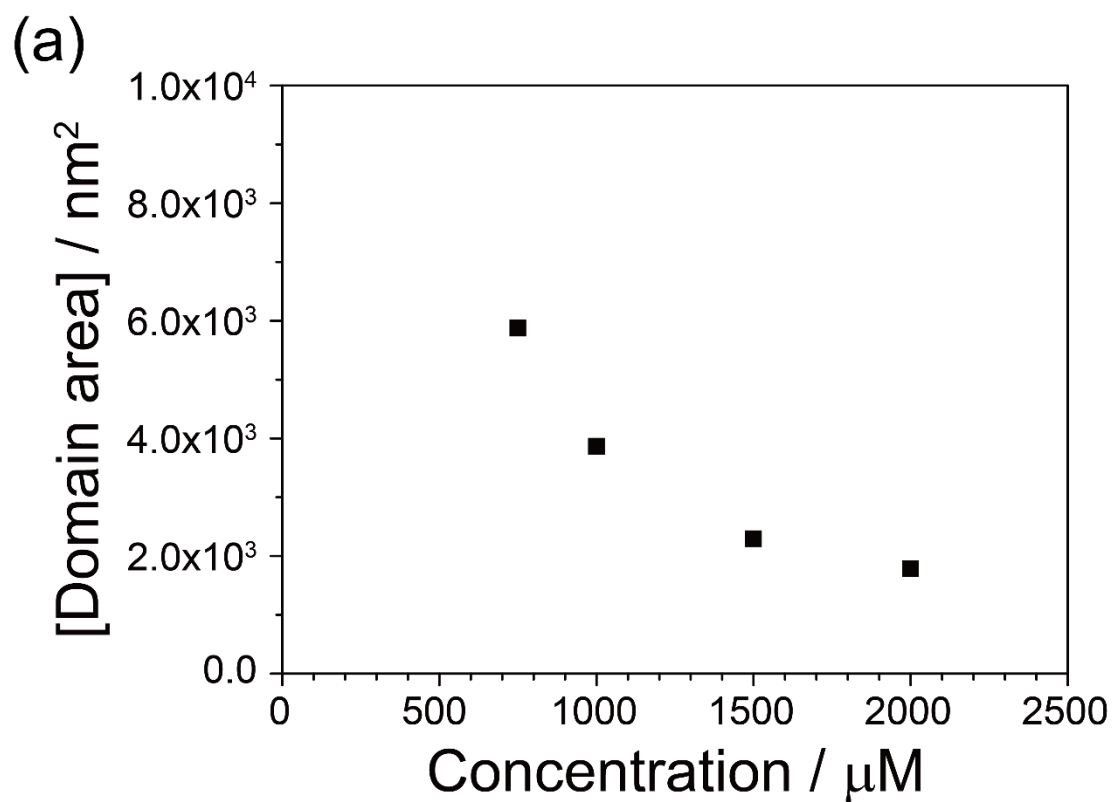


Fig. S7 (a) The plot of average of domain area over sample concentration of **1o** at octanoic acid/HOPG interface. (b) The reciprocal of (a) over sample concentration of **1o**.

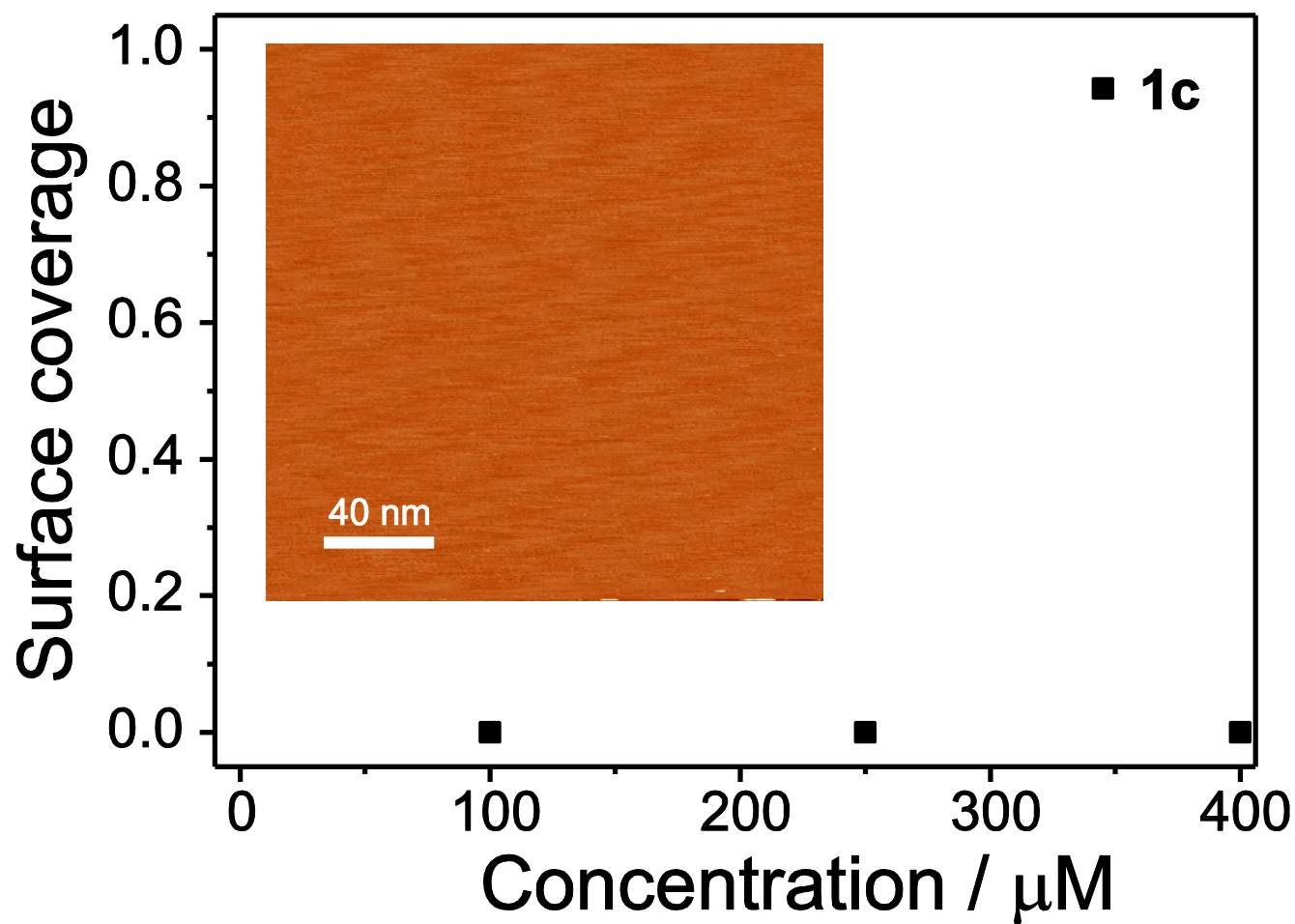


Fig. S8 Concentration dependence of the fractional coverage of **1c** at the octanoic acid/HOPG interface. No ordering of **1c** was observed at various concentrations ranging from 100 to 1000 μM . The inset shows a typical STM image with the closed-ring isomer **1c**.

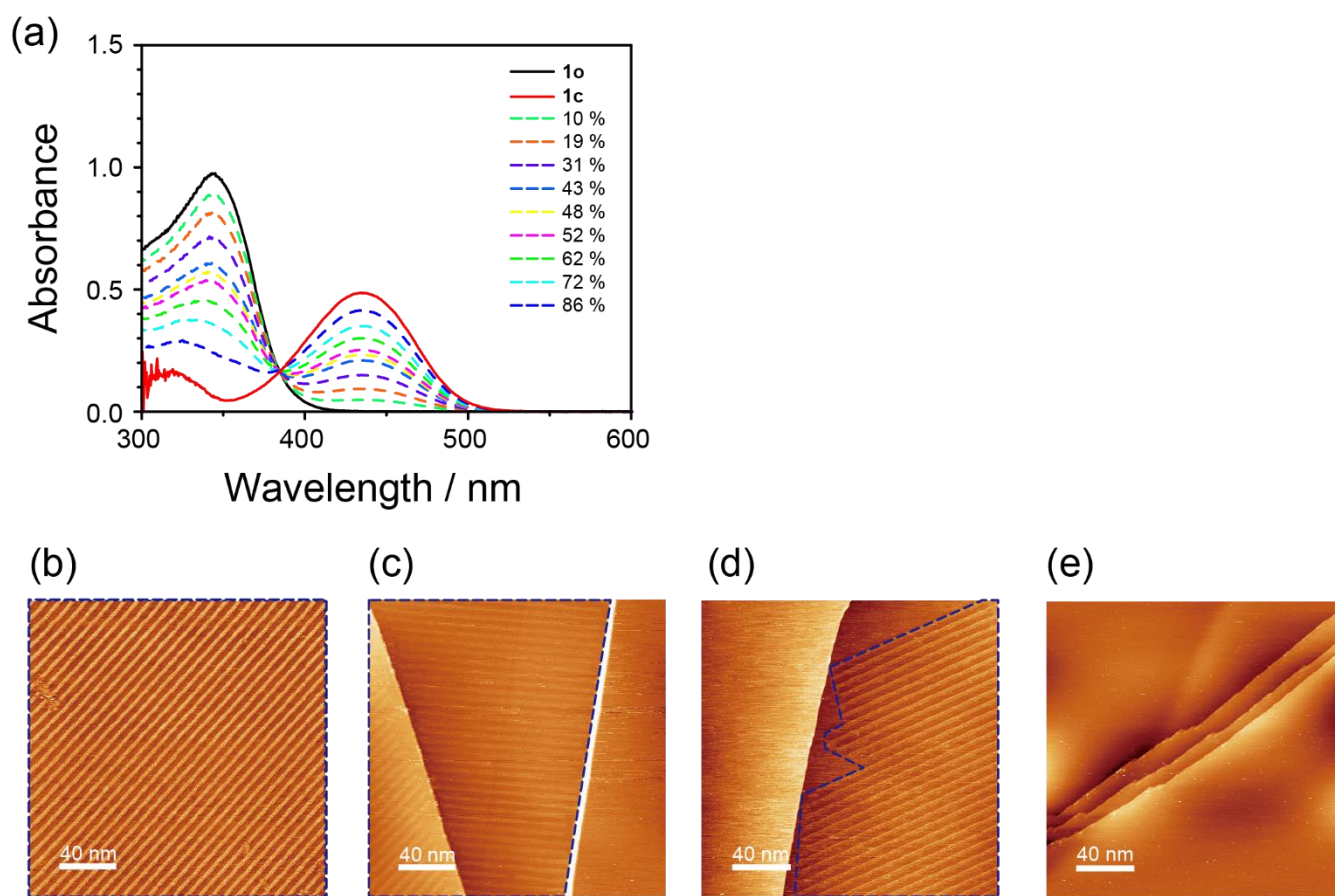


Fig. S9 (a) UV-vis spectral change of **1o** in octanoic acid upon UV irradiation (365 nm). The conversion ratio of **1c** to **1o** for each spectra were shown in the legend. STM images of the sample with conversion ratio (b) 0, (c) 43, (d) 48, and (e) 62 %.

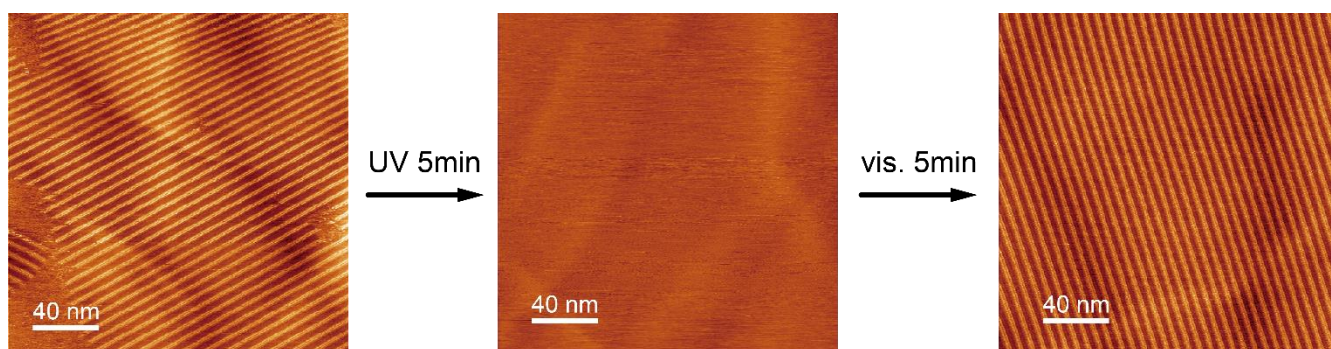


Fig. S10 Reversible ordering formation/disappearance of **1** upon in situ photoirradiation at the octanoic acid/HOPG interface ($c = 500 \mu\text{M}$, $I_{\text{set}} = 30 \text{ pA}$, $V_{\text{bias}} = 800 \text{ mV}$). In situ UV irradiation for 5 min at the liquid/HOPG interface of **1o** solution caused disappearance of the ordering. After the monolayer of **1o** disappeared, visible light irradiation for 5 min to the same sample caused formation of the same monolayer again. These molecular packing of the monolayer was identical before and after photoirradiation.

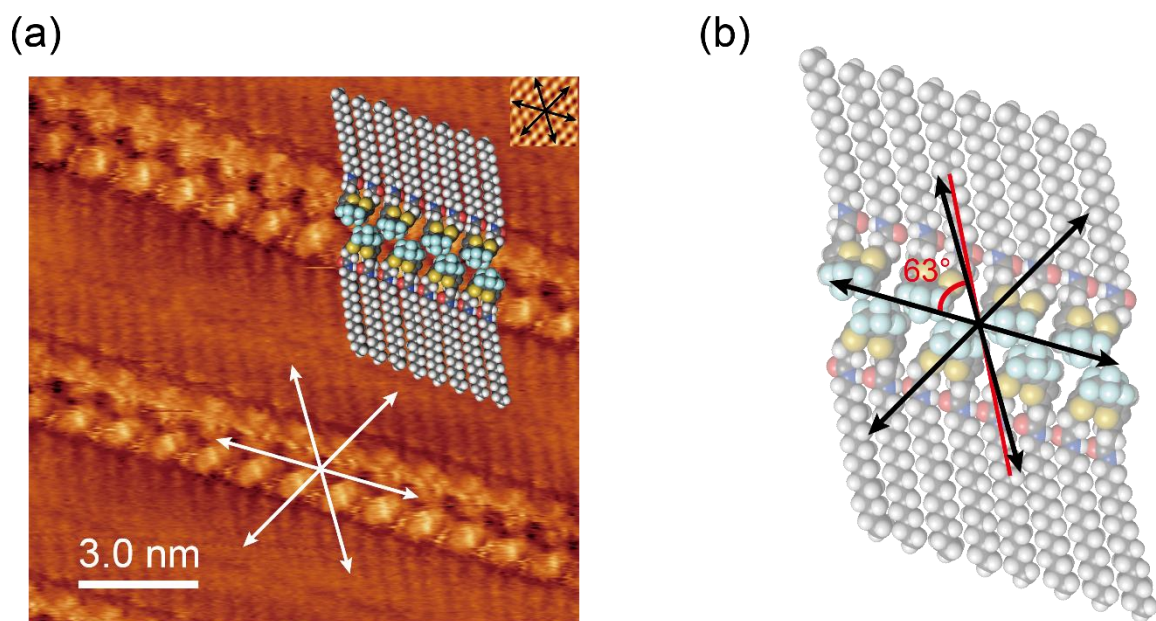


Fig. S11 Molecular orientation in respect to the HOPG lattice. (a) STM image and the direction of HOPG lattice. (b) Molecular model and the direction of HOPG lattice. Arrow shows $\langle 11\bar{2}0 \rangle$ direction of HOPG lattice. Red line shows the direction of alkyl group of diarylethene **1o**. The column of diarylethene and amide group was consistent with $\langle 11\bar{2}0 \rangle$ direction of HOPG. In addition, the direction of alkyl group was tilted at only 3° in respect to $\langle 11\bar{2}0 \rangle$ direction of HOPG, resulting in bright image of alkyl group.

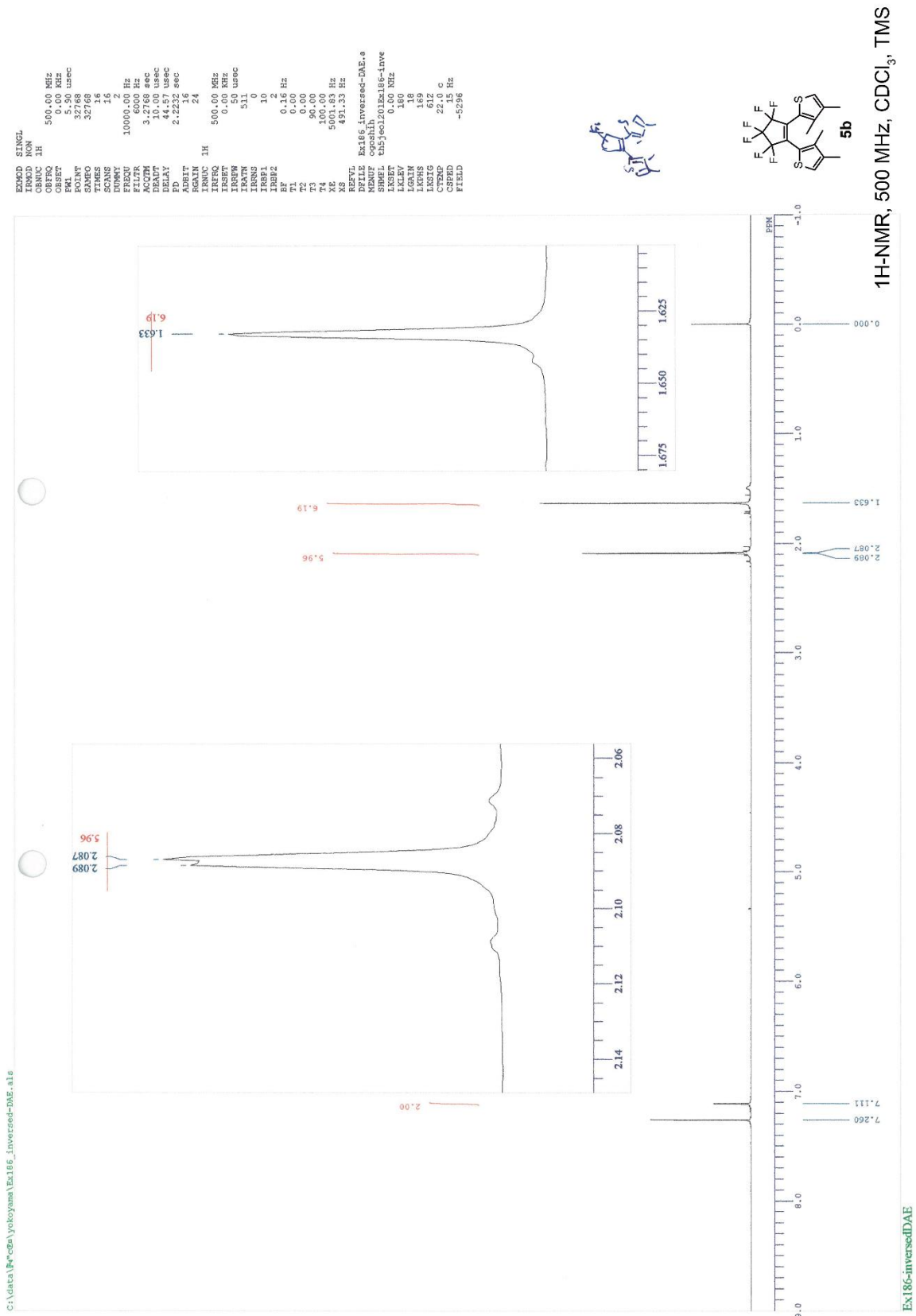


Fig. S12 ¹H NMR spectra of compound **5b** (CDCl₃, 500 MHz)

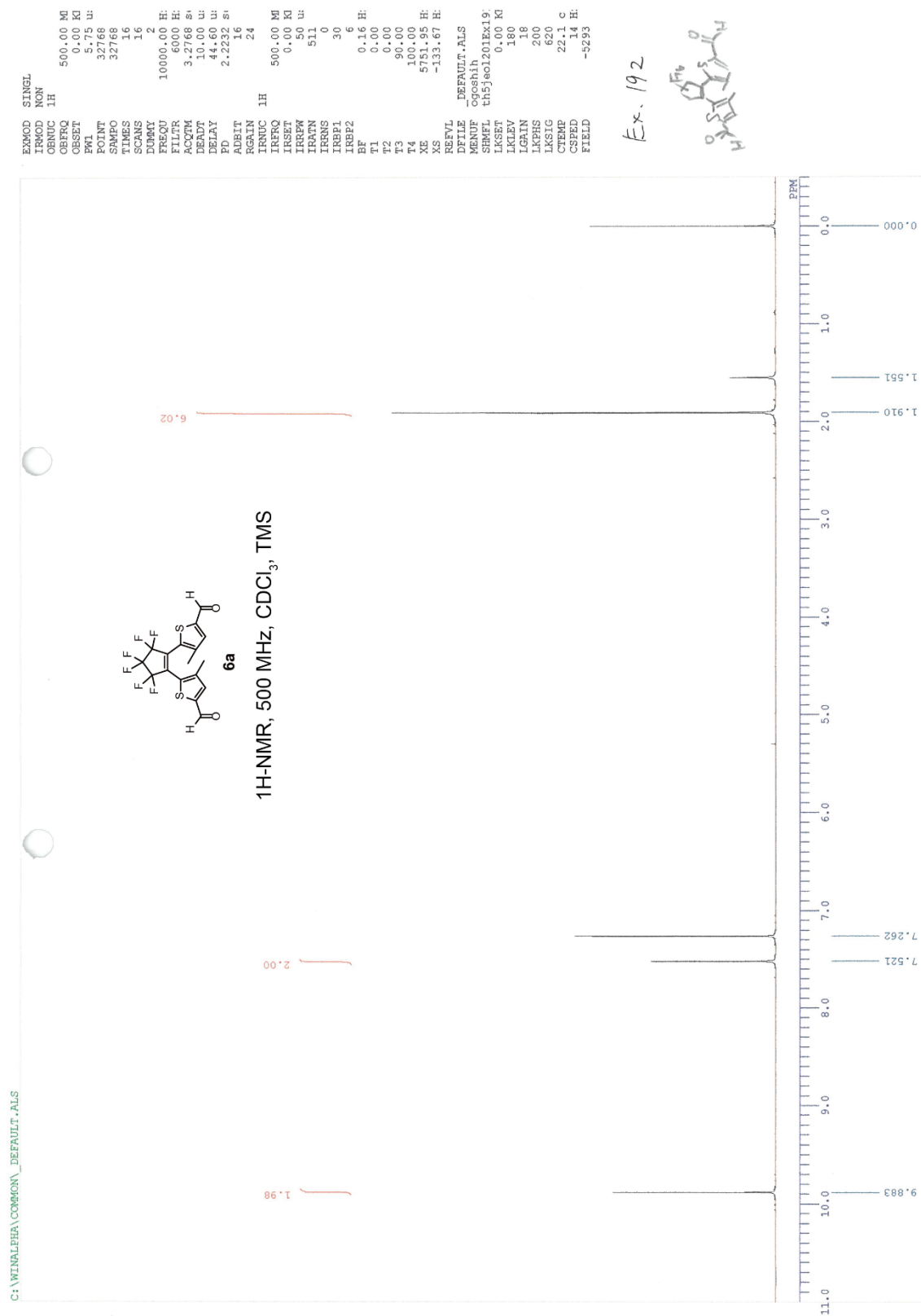


Fig. S13 ¹H NMR spectra of compound **6a** (CDCl₃, 500 MHz)

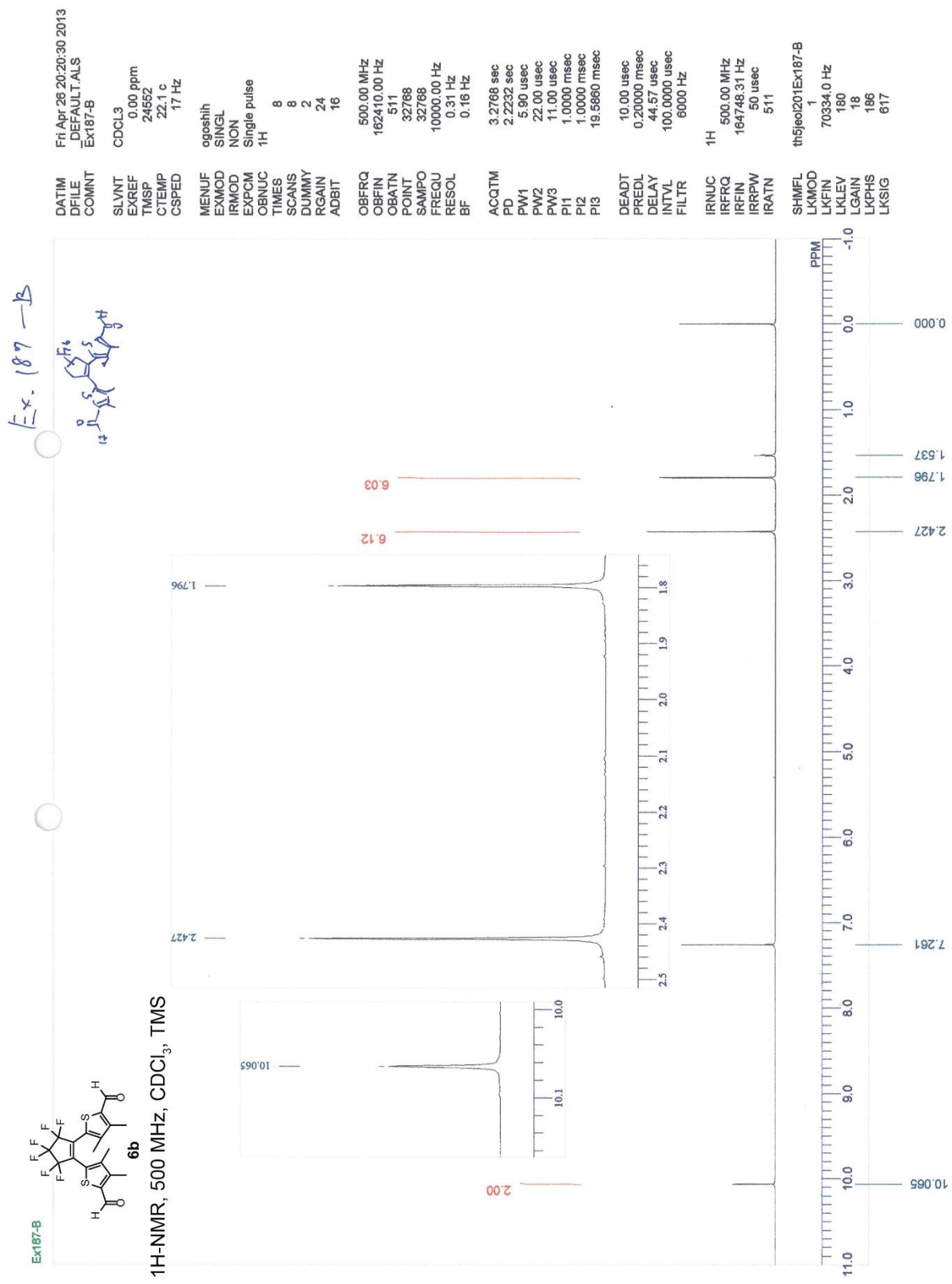


Fig. S14 ¹H NMR spectra of compound **6b** (CDCl₃, 500 MHz)

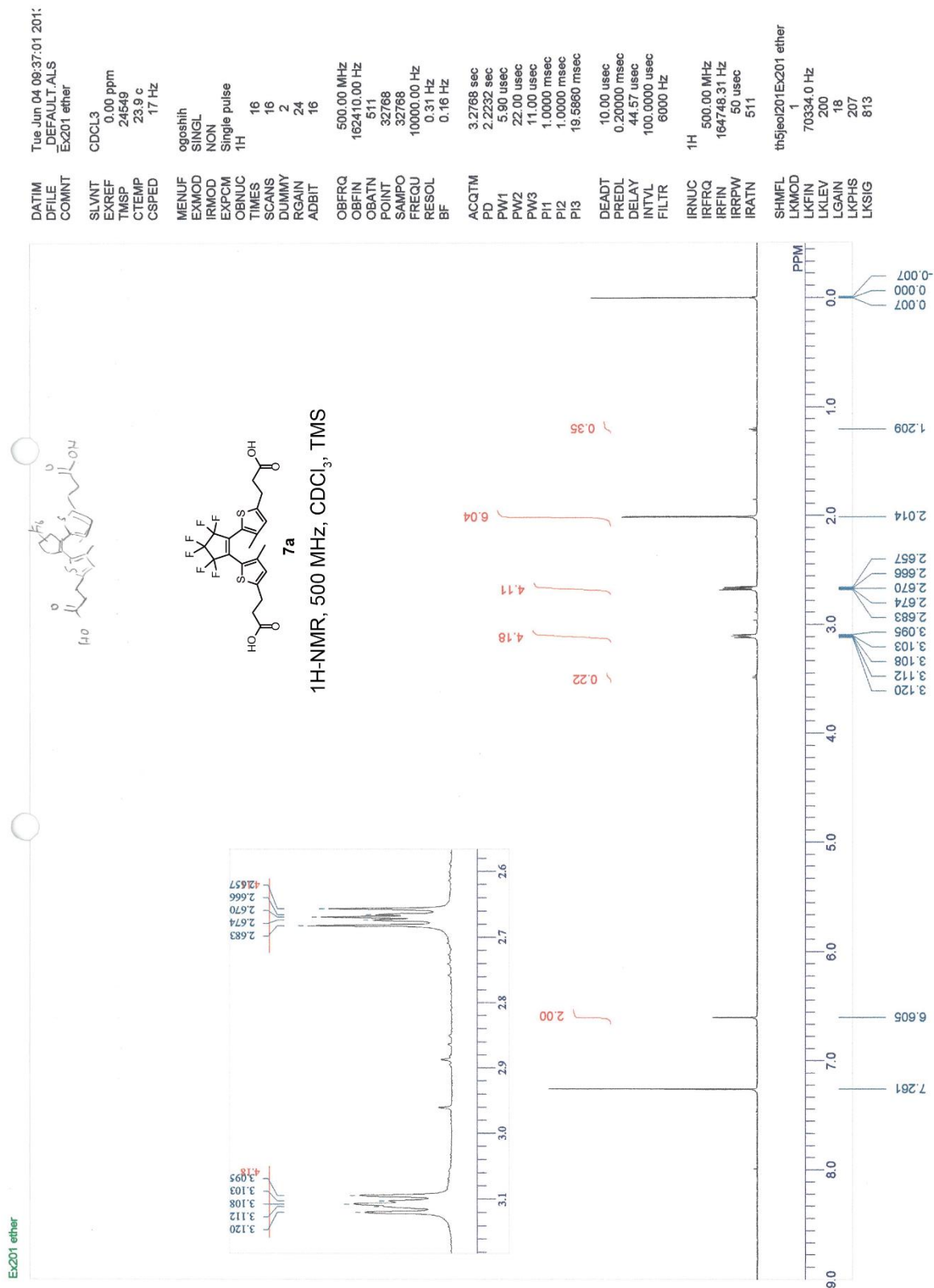


Fig. S15 ¹H NMR spectra of compound **7a** (CDCl₃, 500 MHz)

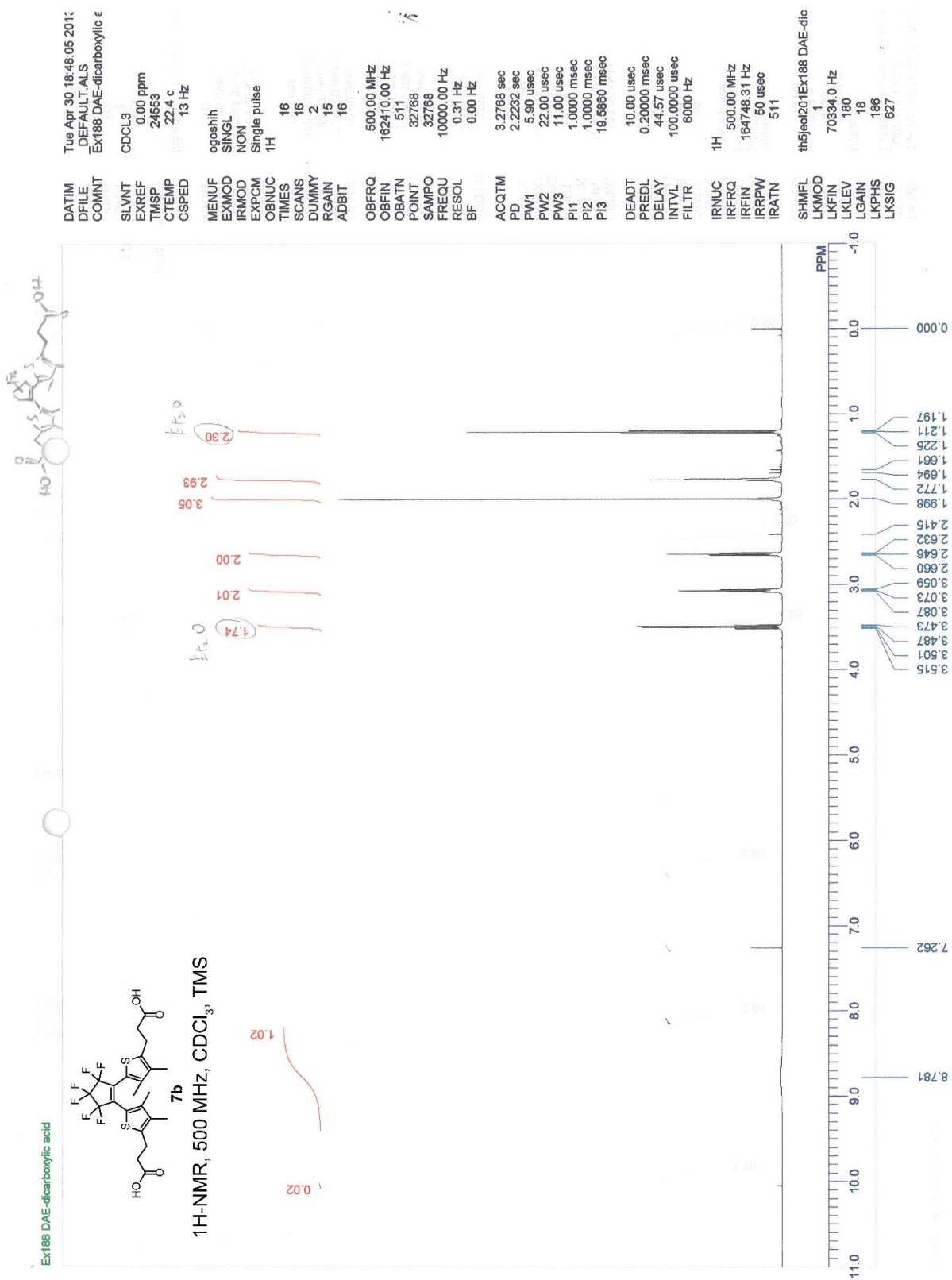


Fig. S16 ¹H NMR spectra of compound **7b** (CDCl₃, 500 MHz)

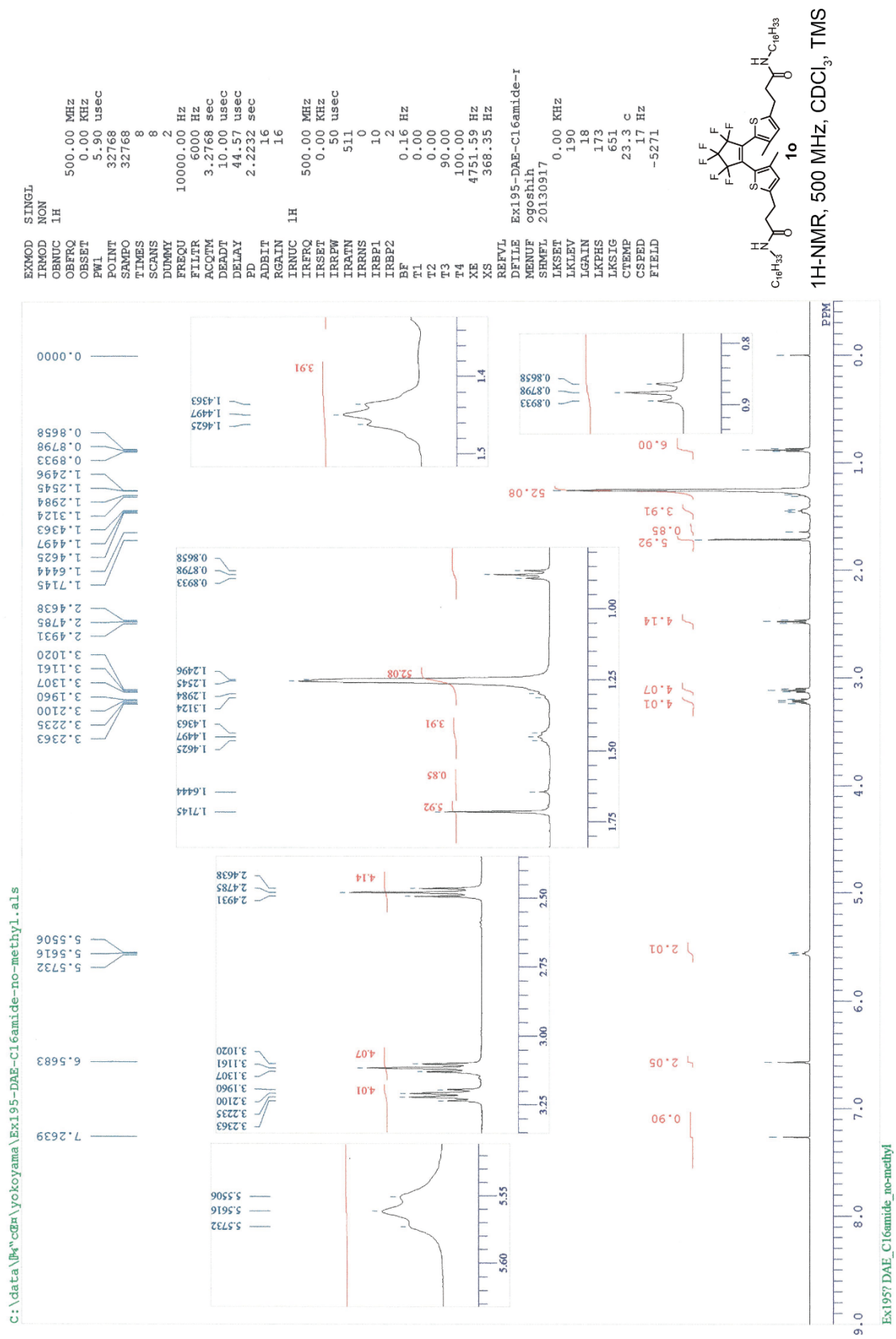


Fig. S17 ¹H NMR spectra of compound **10** (CDCl₃, 500 MHz)

DEFILE EX195DAEAMIDDEC16-13C-1H.aals
 COMNT 2013-10-31 02:46:52
 DATIM 13C
 ORNLIC single pulse dec
 EXMOD 150.97 MHz
 ORFRO 8.52 KHz
 ORSET 1.74 Hz
 POINT 32768
 SCANS 41666.67 Hz
 FREQOU 15000
 ACQTM 0.7864 sec
 PD 1.6200 sec
 PW1 3.77 usec
 IRNUC 1H 24.0 c
 CTEMP CDCl3
 SLVNT 77.00 ppm
 EXREF 0.63 Hz
 BF 60
 RGAIN

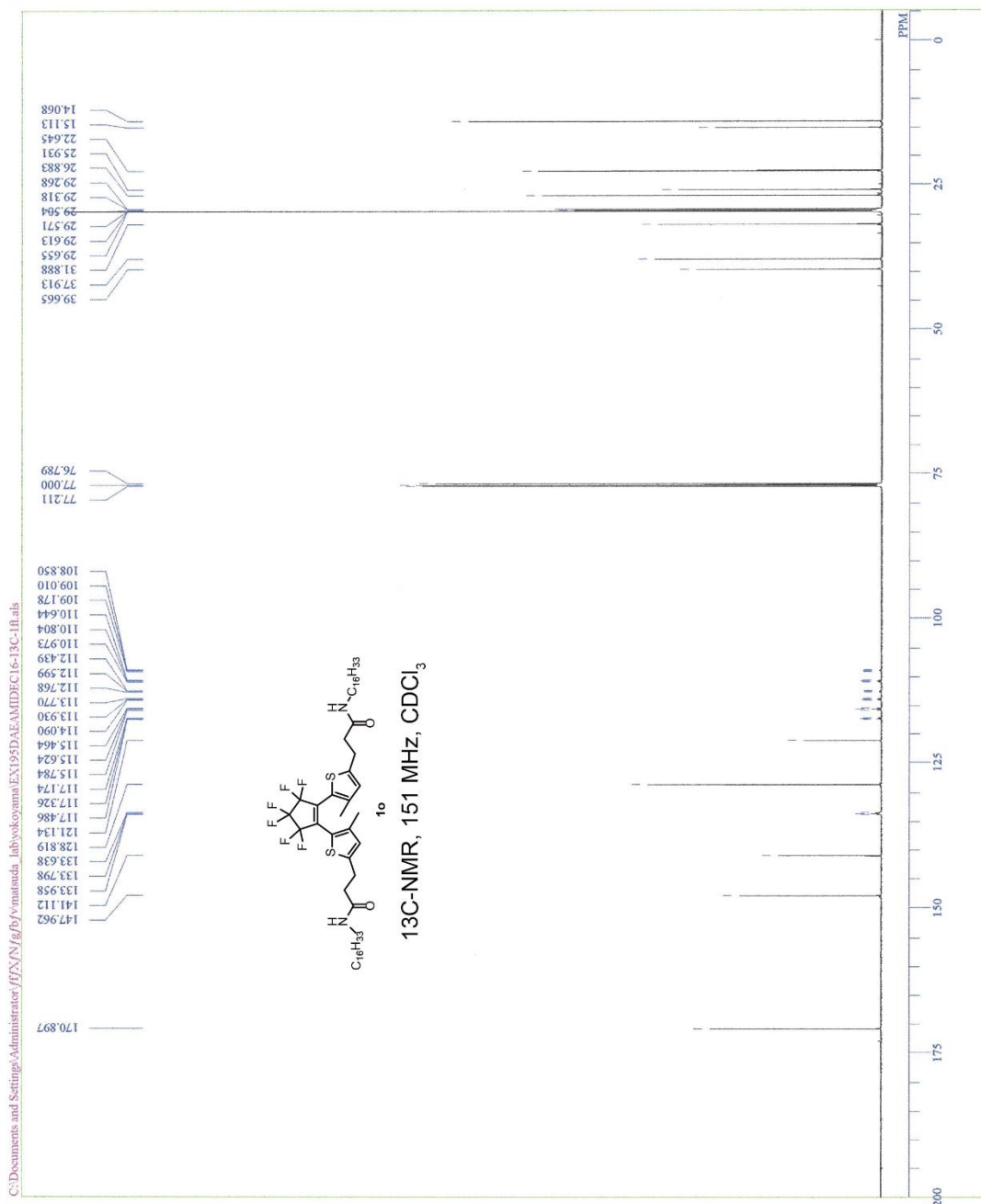


Fig. S18 ¹³C NMR spectra of compound **1o** (CDCl₃, 151 MHz)

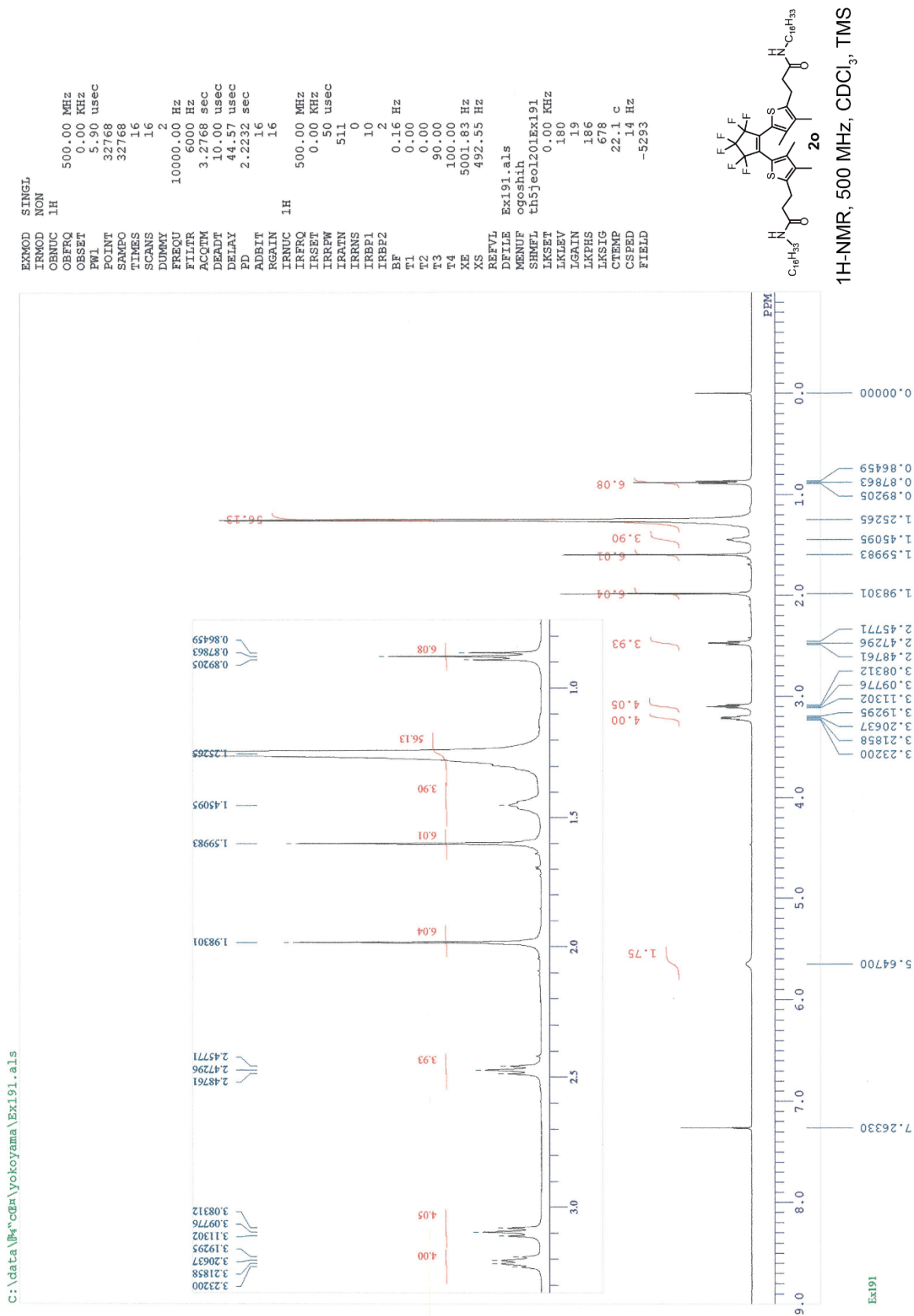


Fig. S19 ¹H NMR spectra of compound **2o** (CDCl₃, 500 MHz)

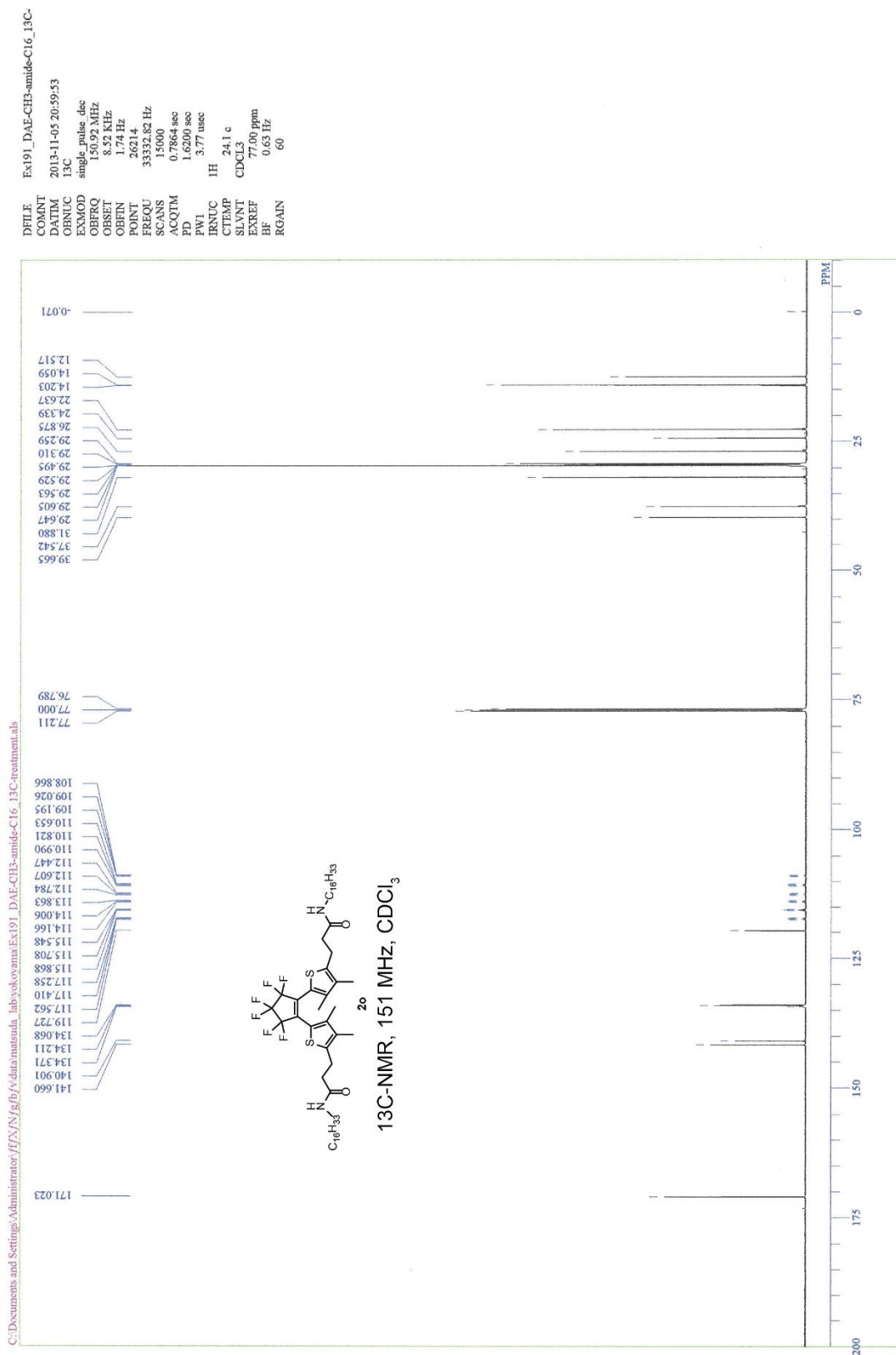


Fig. S20 ¹³C NMR spectra of compound **2o** (CDCl₃, 151 MHz)

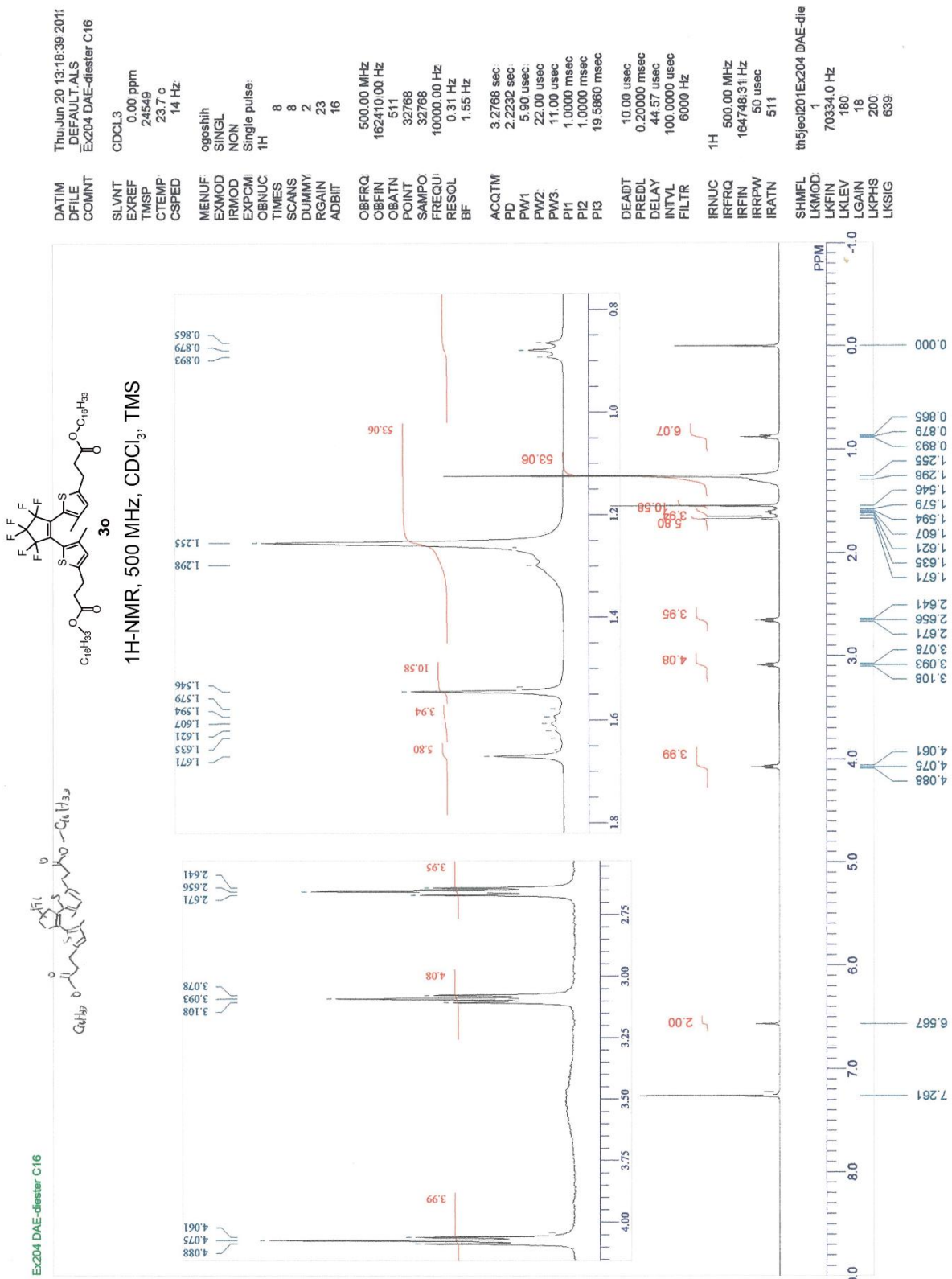


Fig. S21 ¹H NMR spectra of compound **3o** (CDCl₃, 500 MHz)

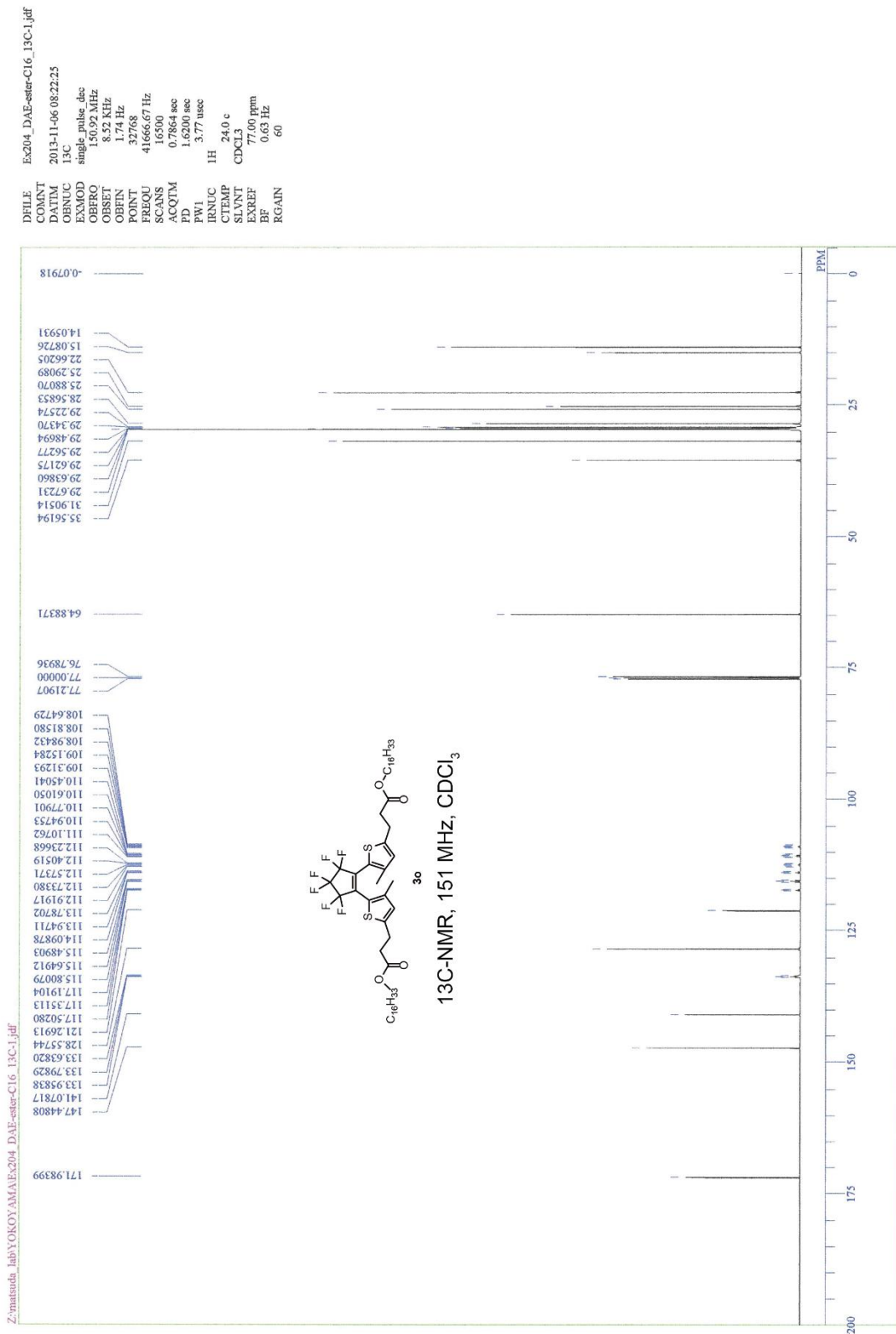


Fig. S22 ¹³C NMR spectra of compound **3o** (CDCl₃, 151 MHz)

C:\data\l\l\yokoyama\closedDAEamide\c16.a1s

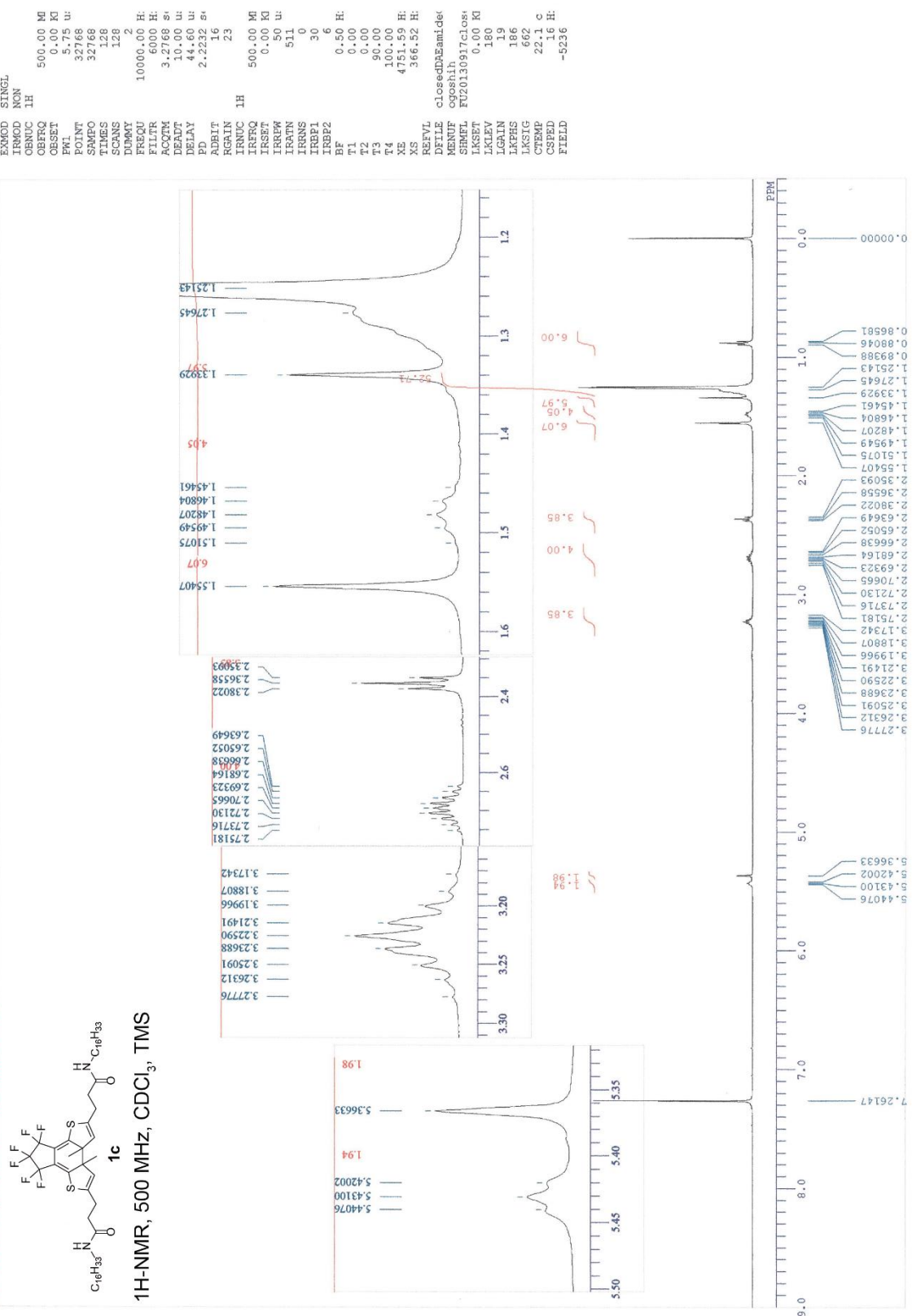


Fig. S23 1H NMR spectra of compound **1c** ($CDCl_3$, 500 MHz)

References

- [S1] S.-R. Deng, T. Wu, G.-Q. Hu, D. Li, Y.-H. Zhou and Z.-Y. Li, *Synth. Commun.*, 2007, **37**, 71.
- [S2] T. Fukaminato, T. Kawai and M. Irie, *Proc. Jpn. Acad. Ser. B*, 2001, **77**, 30.
- [S3] G. Tóth and K. E. Kövér, *Synth. Commun.*, 1995, **25**, 3067.
- [S4] D. Zhao and J. S. Moore, *Org. Biomol. Chem.*, 2003, **1**, 3471.